DESIGN OF A MICRO-HYDROKINETIC ELECTRIC POWER GENERATION SYSTEM

By

Rui Han

RECOMMENDED:

Advisory Committee Chair

Chair, Department of Electrical & Computer Engineering

APPROVED:

Dean, College of Engineering and Mines

Dean of the Graduate School

Aug 24, 2011

Date

DESIGN OF A MICRO-HYDROKINETIC ELECTRIC POWER GENERATION SYSTEM

A

THESIS

Presented to the Faculty

of the University of Alaska Fairbanks

in Partial Fulfillment of the Requirements

for the Degree of

MASTER OF SCIENCE

By

Rui Han, B.S.

Fairbanks, Alaska

August 2011

Abstract

The objective of this thesis project is to design a Micro-Hydrokinetic Power Generating (MHPG) system to generate electricity from sustainable and distributed hydrokinetic resources. The system is developed from a patent held by one of our team members, Robert Kallenberg. The MHPG does not require a dam or diversion, thus avoiding the negative environmental impacts associated with dams. The project could also help some communities to make use of their locally available hydrokinetic resources and significantly reduce their electricity costs.

Reviewing of the literature in hydrokinetic electric power generation technology shows that hydrokinetic projects developed to date have largely made use of hydro turbine systems. These hydro turbines have a strong potential to cause fish mortality, while by design, the MHPG has little chance of causing mortality due to its gentle motion. On the other hand, the build-up of debris on a conventional hydro turbine can easily disable or even destroy the turbine, while the hydro foil in our device is generally oriented with the angle of attack less than 30 degree from the current, keeping debris build up at a minimum.

The state of the art software COMSOL Multiphysics has been used as our numerical analysis tool. The interaction of water and the designed foil in a straight rectangular turbulent channel is modeled, explicitly, using two conservation laws: conservation of momentum and conservation of mass. The incompressible Navier-Stokes application mode in COMSOL Multiphysics has been used in this simulation to solve the distribution of the pressure and the velocity filed. Results show that the oscillating hydro foil has the potential to surpass the efficiency of a conventional turbine, and is deployable in relatively low velocity streams. Future project development suggestions will be presented focusing on further improvements electric machinery design and system integration.

Finally, the prototype of the device has been fabricated and tested in natural rivers. The first test in Chena River, AK, verified the design by showing that the prototype can move in an oscillating manner. The second test in San Gabriel River, CA, shown that the designed Scotch Yoke, which was used to convert linear motion into rotational motion, could be efficiently integrated with the motion generation system. Future test work including permanent magnetic generator coupling and energy efficiency measurement need to be carefully studied concerning the system efficiency and maintenance.

Table of Contents

List of Figures

List of Tables

Acknowledgements

Working on my Master's thesis has been a learning experience, albeit a rewarding one. When I began this project, which requires knowledge not only in Electrical Engineering but multiple skill sets in many engineering fields, I simply had no idea how to approach this research topic and go about answering the key questions. I would like to thank my co-advisors Dr. Jessica Cherry and Dr. Seta Bogosyan for showing me how to pursue this interdisciplinary research. They have always been a source of encouragement, helping me see the big picture of the project instead of only focusing on a small aspect of it. Dr. Cherry and Dr. Bogosyan also spent a lot of their time and energy in guiding me toward writing appropriately in an academic environment. I would like to express my gratitude towards Dr. Cherry for her financial support on my Research Assistant position at International Arctic Research Center and her support for the project and travel expenses.

I would like to thank Dr. Vikas Sonwalkar for his guidance in my Master's coursework and willingness to serve as a committee member for my Master's thesis. I would like to thank Mr. Robert Kallenberg for his work and suggestions about the oscillating hydrofoil prototype we fabricated for testing. Regular meetings with him helped me see how the oscillating hydrofoil system came about as a patent. I would like to thank Mr. Robert Palmer, who helped us manufacture the Scotch Yoke system and provided many valuable ideas for the thesis project. I would like to thank Mr. Gregory Shipman, Mr. Philip Woodard, and Mr. Dale Pomraning from the UAF Geophysical Institute machine shop, for their assistance in putting together the final prototype. I would also like to thank my parents for their constant support.

I hereby acknowledge salary support from the National Science Foundation (NSF) Cooperative Agreement with the International Arctic Research Center grant number ARC-0652838 and salary, travel, and materials support from Alaska EPSCoR NSF award grant number EPS-0701898 and the State of Alaska.

Chapter 1
Introduction

With today's environmental concerns and the predicted resources depletion, the "Going Green" trend has found its way to the forefront of daily life by acting as an aid for improving efficiency, reducing emissions, and saving money. As a relatively new green technology, hydrokinetic energy could also save energy expenses.

In this chapter, current trends in sustainable energy are first discussed. Then the concept of hydrokinetic power is briefly introduced and the potential for hydrokinetic power generation in United States is reviewed. The subsequent section discusses the role of renewable energy in Alaska, focusing on the dilemma of energy supply and demand, including why the state's possession of vast oil and natural gas resources hardly reduce the energy bill for most of the local communities, and the state government policy towards renewable energy development. Followed by this is an introductory explaination of how our device will work in flowing water. Lastly, the author's contributions to the hydrokinetic power generation technology and clean energy development are described.

1.1 Why Sustainable Energy

The end of the fossil fuels age may be in sight, but the question of what will come after it is still open. There are numerous energy alternatives to coal, oil, and natural gas, including electricity generated by hydrokinetic energy and biofuels extracted from plants. Scaling up these alternative sources of energy, however, has proved to be a challenge.

According to the Energy Information Authority's (EIA) 2010 projection[1], even though the U.S. economy is rapidly growing in the less *energy-intensive*[1] service sectors, and as the efficiency of energy-consuming appliances, vehicles, and structures improves, there is strong growth in energy use to generate electricity and to produce liquid fuels for the transportation sector. With the development of unconventional vehicles (vehicles that use alternative fuels, electric motors and advanced electricity storage, advanced engine controls, or other new technologies), the growth in energy consumption to generate electricity is greater than the EIA projected.

In 2008, 19% of global energy consumption came from renewable resources, which include traditional biomass, large hydropower, small hydro, modern biomass, wind, solar, geothermal, and biofuels (Figure1.1) [2]. The share of renewables in electricity genera-

[1]measured as the amount of energy consumed per dollar of gross domestic product (GDP) of U.S..

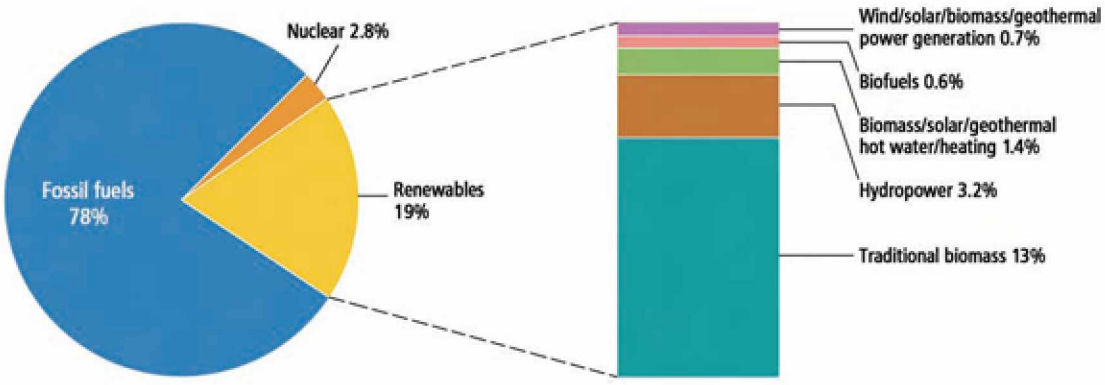

Figure 1.1. Renewable energy share of global final energy Consumption[1]

tion is around 18 %, with 15% of global electricity coming from hydroelectricity and 3% from new renewable, such as photovoltaics, biomass, and geothermal. Existing renewable power capacity worldwide reached an estimated 1,230 gigawatts (GW) in 2009, up 7 percent from 2008. Renewable energy now comprises about a quarter of the global power-generating capacity (estimated at 4,800 GW in 2009) and supplies some 18 percent of global electricity production. For hydropower, it has been growing annually by about 30 GW in recent years [2, 3].

Many renewable energy projects that have been developed are large scale projects. However, downsized small scale renewable technologies are well suited to small remote communities, such as those in Alaska, where energy is often crucial in human development. In fact, Alaska rural communities rely primarily on diesel electric generators for power and may pay more than \$1/kWh. This is because Alaska's electricity infrastructure differs from the lower 48 States in that many consumers are not linked to large interconnected grids through transmission and distribution lines. Therefore harnessing the local available renewable energy resources, such as hydrokinetic power and wind power, is of paramount importance in solving the energy crisis in rural Alaska.

Scaling up renewable resources such as sunlight, wind, tides, plant growth, and geothermal heat to meet the long time energy projections can not only ease the impact of price fluctuation of fossil fuels, but also reduce the greenhouse gas emissions. Increasing the share of renewables, globally, will results in significantly lower greenhouse gas emissions.

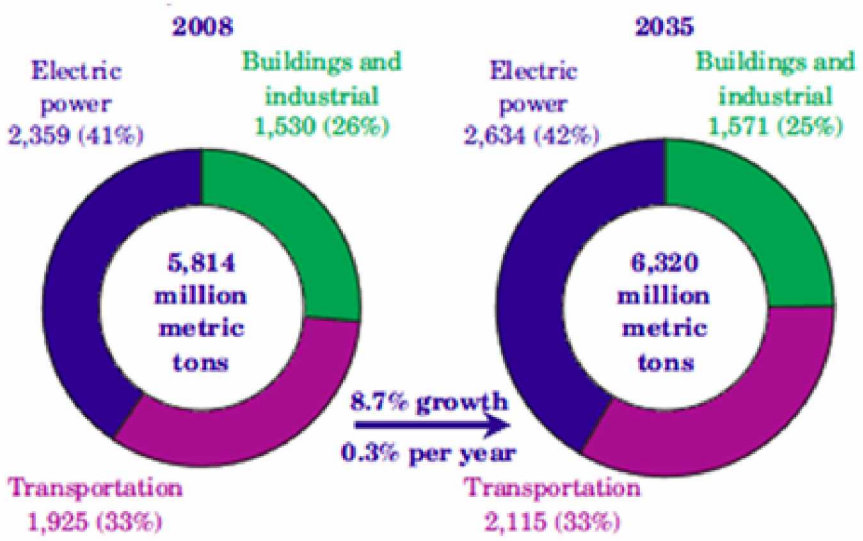

Figure 1.2. U.S. energy related carbon dioxide emission, 2008 and 2035 [1]

In the EIA's Reference Case[2], CO_2 emissions from energy grow on average by 0.3 percent per year from 2008 to 2035, or a total of 9 percent. Most of the growth in CO_2 emissions in the [1] reference case is accounted for by the electric power and transportation sectors as shown in Figure 1.2. Replacing fossil fuels also has positive air quality benefits. These are especially positive in the electricity and transportation sectors.

1.2 The History of Hydropower

The power of tidal, river and ocean currents and ocean waves is tremendous, and the basic concept to make use of these in the form of hydropower is not new. For centuries people have harnessed the power of river currents by installing water wheels of various sorts to turn shafts or belts. For example, Ancient Greece used the energy in falling water to generate power to grind wheat by installing water wheels. In the American colonies, undershot waterwheels were built so that only the bottom of the wheel was in the river, drove flour and lumber mills. Dams and diversions, which are required for conventional hydroelectric but not for hydrokinetic power, were built across rivers in the United States to power mills and factories throughout the 19th and 20th centuries.

Modern ocean wave energy conversion machines use new technology that is designed to operate in high amplitude waves, and modern tidal/river/ocean current hydrokinetic

[2]Assumes no explicit regulations to limit GHG emissions beyond the recent vehicle GHG standards

machines use new technology that is designed to operate in fast currents. Both of these emerging technologies have the potential to provide significant amounts of affordable electricity with low environmental impacts given proper care in siting, deployment, and operation.

1.3 The Role of Hydrokinetic Power Generation

Hydrokinetic power generation refers to technologies that generate renewable electricity by harnessing the kinetic energy of a body of water, such as waves, tides, ocean, and in-stream river currents. The power of moving water is obvious to anyone who has stood in breaking waves or struggled to swim against a river's current. New technologies can enable us to harness the power of moving water without building new dams that can have major impacts on wildlife and water quality.

Hydrokinetic energy has great potential to be explored in the U.S.. Estimates suggest that the amount of energy that could feasibly be captured from U.S. waves, tides and river currents is enough to power over 67 million homes [4]. Based on current project proposals, experts predict that the country could be producing 13,000 MW of power from hydrokinetic energy by 2025 [5]. This level of development is equivalent to 22 new dirty coal-fired power plants - avoiding the annual emission of nearly 86 million metric tons of carbon dioxide, as well as other harmful pollutants like mercury and particulate matter. The avoided carbon emissions in 2025 would be equivalent to taking 15.6 million cars off the road [6].

As the concept of generating profitable electricity from hydrokinetic power resources has been studied and proved feasible over the years, a significant number of project proposals have been developed. Over a hundred conceptual designs of hydrokinetic devices have been developed worldwide. As of 2009, the United States Federal Energy Regulatory Commission (FERC) has issued 146 preliminary applications to study development of 9,000 MW in proposed hydrokinetic generation, however, only a few of these have been tested and operated at full-scale [7] (See Figure 1.3). Generally, for most of the hydrokinetic projects, there are three challenges that prevent them from being fully developed into commercial technologies. The first challenge is that the it is hard to simulate the fluid structure interaction numerically, lacking theoretical verification of the feasibility before putting into practice; one example is the "Stingray" project [8, 9, 10]. The second challenge is that most devices obstruct navigation or diminish the value of coastal real estate.

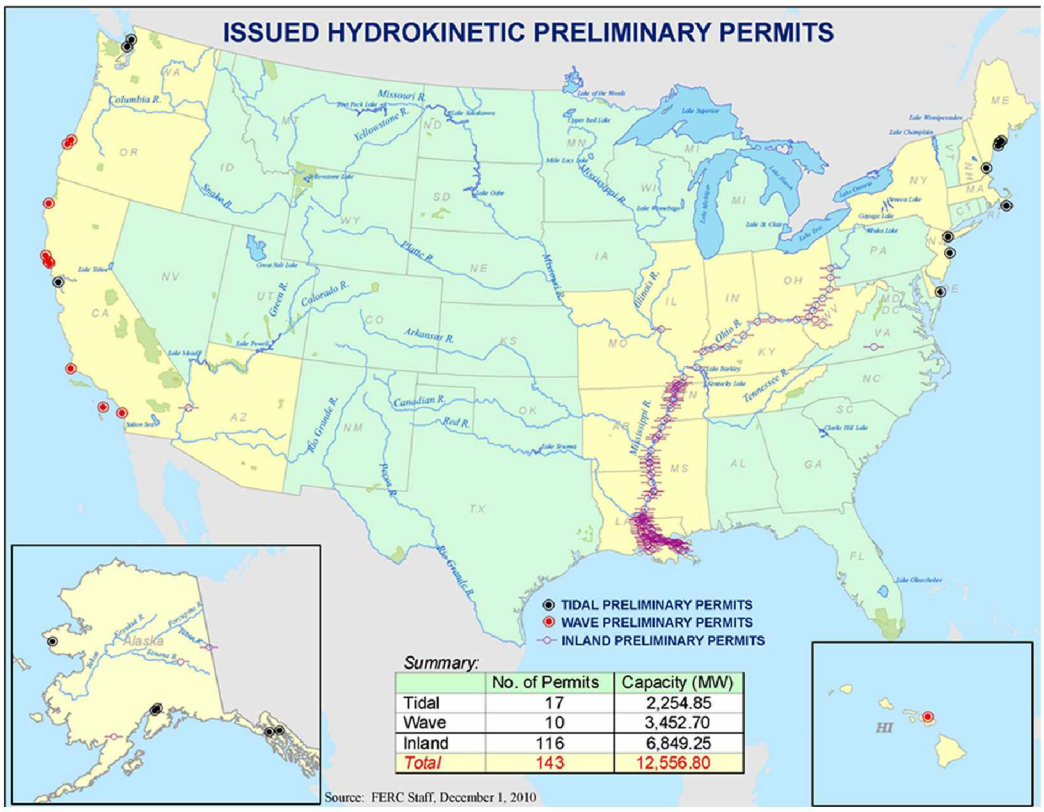

Figure 1.3. Issued hydrokinetic preliminary permits (December 1, 2010)

Last but not least, most of the above mentioned hydrokinetic devices are not friendly to marine life and suffer from debris attack because almost all of them harness the hydrokinetic energy by rotational blades configured vertically or horizontally in the water. The debris attack problem can dramatically decrease the operational lifetime or even destroy the energy harvest system. Due to the above mentioned challenges, we need to find a technology that is reliable, friendly to marine life and protected from debris accumulation, and does not create conflict in navigating in the same water areas. In this case, the innovative hydrokinetic energy harvest device described herein provides solutions to some of these problems.

1.4 Renewable Energy in Alaska

1.4.1 The Dilemma of Energy Supply and Demand in Alaska

Alaska has vast energy resources. According to the Energy Information Administration, Alaska ranks second in the nation in crude oil production. Prudhoe Bay on Alaska's North Slope is the highest yielding oil field in the United States and on North America, typically producing about 400,000 barrels per day. However, Alaska residents are struggling with high energy prices with these costs representing a very large portion of living expenses. They have the highest per capita energy use in the nation due to the long, cold winter climate. In Alaska, the three major components of energy use are: space heating, electricity, and transportation. Most of the remote communities depend on diesel generation. Barges may only deliver fuel two or three times during the year (summer only) and the costs are exorbitant.

Alaska's unique geographical location and low population density have driven the development of its energy supply infrastructure. Alaska has over 150 remote, stand-alone electrical grids serving villages as well as larger transmission grids in the southeast part of the state and the Railbelt, between Fairbanks and Anchorage. The Anchorage and Railbelt area have enjoyed relatively low-cost heating and power since expansion of the Eklutna hydro plant in 1955 and the development of major Cook Inlet oil and gas discoveries in the 1960s. It is predominately the small and more remote communities that pay the highest prices for power. These same communities are also likely to have high food costs and limited jobs available.

Fortunately, Alaska is also a state with abundant renewable energy resources, including wind and hydro resources. Many of those rural communities are either situated along

navigable rivers that could host hydrokinetic installations or in the middle of windy regions that can take advantage of wind power. The already developed tidal energy project at Cook Inlet could tremendously increase the power production for the Alaska Railbelt power grid.

According to the investigation conducted by the Alaska Center for Energy and Power (ACEP), Alaska has about 40% of the total U.S. river energy resource potential and about 90% of the total U.S. tidal energy resources [11]. In 2009, hydroelectric power plants with dams supplied 24% of the state's electrical energy. There are 37 hydro projects providing power to Alaska utility customers. The 126 MW state owned Bradley Lake project supplies 8% of the Railbelt. The 6 MW Blue Lake project near Sitka supplies 60 percent of Sitka's average electricity requirements; and the proposed 330 MW Lake Chakachmna project , located 85 miles west of Anchorage, would supply power to the Railbelt grid using lack tap and a 10 mile tunnel [12].

Many rural communities located on the Yukon and other large rivers are interested in using river currents for generating power. This technology is the major topic of this thesis, which is technically termed as hydrokinetic electrical power generation or in-stream electrical power generation. In the summer of 2008, the community of Ruby and the Yukon River Intertribal Watershed Council installed a 5 kW experimental river current turbine, the first in-stream water turbine ever deployed in the nation, to test feasibility of in-stream power generation on the Yukon River. This project team plans to continue testing a 5kW and eventually a 25kW turbine at Ruby. Similarly, Alaska Power and Telephone has issued an RFP for a hydrokinetic device they plan to deploy at Eagle in 2010. The communities of Whitestone and Igiugig are also pursuing hydrokinetic projects. Another project proposed by Ocean Renewable Power Company (ORPC) is seeking a permit from the Federal Energy Regulatory Commission to deploy their pilot hydro turbines at Nenana. This turbine would be bigger than the Ruby project, which rated from 50 to 300 Kilowatts depend on the flowing speed. This system is scheduled to be up and running in 2012. Furthermore, the Alaska Center for Energy and Power is developing a test center for hydrokinetic technology at Nenana on the Tanana River.

1.4.2 Alaska Government Policy in Renewable Energy

In January 2009, The Alaska Energy Authority (AEA) and Alaska Center for Energy and Power (ACEP) coproduced a document, "Alaska Energy: a first step toward energy in-

dependence" [13], to encourage communities to review locally available resources and determine the most cost effective energy options for their specific community. The concept "Energy meter" was proposed as an efficient measuring tool to express the needs and availability of the local energy alternatives; it can graphically show the comparison between the different energy solutions based on the range of crude oil price for a community. This report is a key step in connecting all Alaskans to an abundant, affordable, clean, efficient, and reliable electric power network in that: (1) A large number of Alaskan communities have the potential to make use of their local available energy resources, such as wind and hydro power, instead of relying purely on fossil fuels; (2) It is impossible to investigate the alternative energy solutions throughout the state while relying on limited contributions from government agencies, so the goal is more likely to be achieved when supported by communities; (3) By utilizing those potential sustainable energy resources scattered throughout the state, residents can save money on their energy bill and even supply sufficient household energy independent of utilities. Moreover, they can even sell their extra power back to the utility company, in a similar fashion as the SNAP program operated by the Golden Valley Electric Association (GVEA) in Fairbanks, Alaska; (4) Ultimately, the goal is to build an intelligent state wide grid that uses distributed energy resources to serve local loads and to meet specific application requirements for remote power, village or district power, and premium power.

The state government is also committed to the development of sustainable energy technologies. The passage of Senate Bill 220 (SB220), the Alaska Sustainable Energy Act, has turned federal stimulus fund money for renewable energy development of $18milion into a $250 million loan. Schools, municipalities and the state are eligible for loan funds for energy efficiency improvements to buildings. Those amounts of money allow Alaska to make major progress in retrofitting public buildings in a reasonable period of time, resulting in big savings of energy and money. It also states that the Department of Transportation and Public Facilities should make energy efficiency retrofits to at least 25 percent of state buildings 10,000 sq ft and larger by January 1, 2020. Moreover, the bill creates the Emerging Energy Technology Fund to focus on demonstrating new technologies, and allows municipal tax exemptions for "certain residential renewable energy systems".

House Bill 306 (HB 306), the State Energy Policy, was sponsored by the House Special Committee on Energy, and built by a stakeholder working group that included Alaska

Conservation Alliance (ACA[3]). HB 306 marked a turning point in Alaska's years-long progress on renewable energy and energy efficiency. The bill's opening lines cover three of ACA's top energy goals: improve energy efficiency across the state, increase the use of renewable energy sources, and use natural gas as a bridge fuel to a clean energy economy. In addition, the intent of the legislature in HB 306 section 1 stated that: (1) the state achieve a 15 percent increase in energy efficiency on a per capita basis between 2010 and 2020; (2) *the state receive 50 percent of its electric generation from renewable and alternative energy sources by 2025;* (3) the state work to ensure a reliable in-state gas supply for residents of the state. In HB 360 Section 2, the bill also shows the intent of the state to promote energy education and research in that university programs apply energy research and development of alternative and emerging technologies to achieve reductions in state energy costs and stimulate industry investment in the state. Other notable provisions include: Promotes renewable energy resources such as geothermal, wind, solar, hydroelectric, hydrokinetic, tidal, and biomass energy, puts emphasis on the long-term costs savings provided by projects such as hydroelectric and geothermal energy sources with high up-front costs and long-term price stability, and promotes energy efficiency in transportation, etc.

1.5 Oscillating Hydrofoil Power Generation Concept

Our project is based on a novel invention [14] patented by Robert C. Kallenberg in 2001. It is intended to harness the hydrokinetic energy from flowing water in river or streams by deploying a simple oscillating foil. The mechanism had never been used in any other hydrokinetic proposal or project before we started. So far, the turbine is the dominant device investigated in hydrokinetic power generation, and it makes up most of the hydrokinetic literature; other form of energy conversion are described, including oscillating water foils [8, 9, 10, 15, 16], vortex induced vibrations [17], etc. Below we will introduce the patented device, an oscillating hydrofoil for in-stream current. In the chapter 2, we will conduct a literature review regarding the pilot hydrokinetic projects and some other hydrokinetic power generation technology.

Figure 1.4 is the two dimensional motion generating system from the patent [14]. It includes a pivotally disposed hydrofoil and a supporting rod (See Figure 1.4a). The hydrofoil is vertically disposed in flowing water such as a river, and configured to move under hydro-dynamic force, by periodically changing the position of the trim tab at the trailing

[3]http://akvoice.org/home-slot-five/statewide-energy-policy-plan

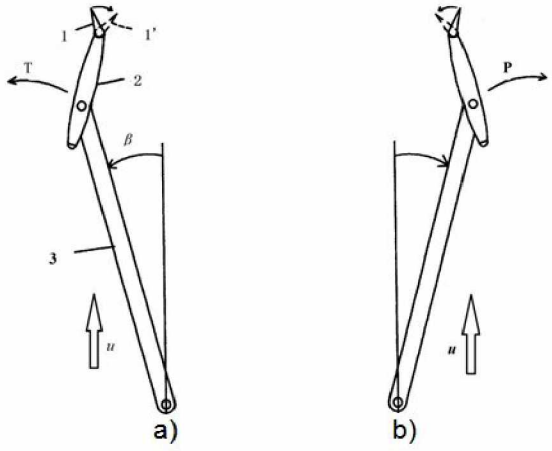

Figure 1.4. 2D Representation of the motion generation system

edge. The foil will be driven by the hydro-dynamic force to move in an oscillating fashion, as does the supporting rod. To generate electrical power, a crank mechanism or Scotch Yoke can be employed to couple the linear motions of the rod and the rotational motions of the rotor in a commercial Permanent Magnetic Generator (PMG).

More specifically, with reference to Figure 1.4a, the rod (Part 3 in Figure 1.4a) will move leftward when the trim tab (Part 1 in Figure 1.4a) is configured in a leftward position as shown. The leftward position of the trim tab causes the foil (Part 2 in Figure 1.4a) to be in a rightward position. Water flowing in the direction from the leading edge of the foil to the trim tab flows against the right surface of the foil, thus the total fluid force acting on the foil's surface will drive the foil and rod moving leftward.

When the rod has reached the most leftward position as indicated by angle β, the trim tab is actuated to pivot rightward as indicated by the dash line (part 1' in 1.4a). Water then flows against the right surface of the actuated rightward trim tap (part 1 in Fig 1.4a), causing the foil to pivot leftward as indicated by arrow "T". Water then flows against the left surface of the foil, thereby the total fluid force acting on the foil will drive the foil moving right as indicated by arrow P and bring along the rod to move rightward. It takes a half period for the harmonic oscillation of the rod to reach the right most position as indicated in 1.4b. The next half period of oscillation will be identical to the previous half period except the phase will be inverted.

1.6 Thesis Contributions

In this thesis, we address the problem of harvesting hydrokinetic energy from in-stream hydro resources by an oscillating hydrofoil system, the core idea of which has never been studied before. This oscillating hydrofoil system has the following appealing characteristics such as high energy density, low maintenance requirement, intact river navigation, friendly to marine habitant, and resistant to debris attack.

The review and comments on both turbine and non-turbine hydrokinetic technologies from all over the world provide a substantial and comprehensive overview of the status and challenges of hydrokinetic power generation. The technology review highlights the benefits of the oscillating hydrofoil technology by comparing this technology and already developed technologies. This review can also be very useful to people who would like work in this area.

The hydrodynamics of hydrofoils have been studied using the Finite Element Menthod (FEM) theory in COMSOL Multiphysics. This unprecedented modeling work is another highlight of this project.

Based on the analysis, a prototype of the oscillating hydrofoil is fabricated by our team members. We built the oscillating generation subsystems the linear-to-rotational conversion system, and the generator integration gear system stage by stage to verify our design and the original ideas of oscillating hydrofoil system.

Chapter 2
Methodology: A Review of Hydrokinetic Resources and Technologies

The objective is to define a process to match the most appropriate technology to a particular river or tidal current resource site and thus produce the maximum energy from the certain amount of resources. The methodology is made up of two main parts: (1) Resource Methodology - Analyzing the resource at the site; (2) Technology Methodology - Analyzing the technology and matching it to the studied resource for the optimal power output. The resource methodology is based on recognizing and defining the characteristics of the site in terms of bathymetry, current velocity and seabed roughness. The study of the resource includes performing an analysis of different technologies and their power output and efficiency for varying flow, allocating power ratings to the devices, evaluating the economic and environmental factors, and in addition, calculating the impact factor for flow velocity. It could be developed with a number of optional evaluation tools that hydrokinetic energy developers can either utilize or replace with their own resources. By better defining the nature of the site, it is more likely that the technology chosen will be the most appropriate for that site and therefore have the optimum combination of efficiency, power output and economic factors.

2.1 Brief Review of Hydrokinetic Resource

There are a number of types of water resources from which it is possible to generate electricity with kinetic energy. The energy contained in ocean waves is believed to have the greatest energy production potential among those options; however, wave technology is more prohibitive to development and deployment than other forms of hydrokinetic resources. In addition to waves, researchers believe that ocean tides are a promising sustainable energy resource. The predictable tidal streams have the potential to provide us with new source of clean electricity without building dams. Moreover, although to make use of in-stream-based hydrokinetic energy is not as evolved as its wave and tidal counterparts, initial estimates expect in-stream-based water resources could fulfill electricity needs for an additional 23 million typical homes [4]. The in-stream hydrokinetic resources prove to be a particularly valuable energy form for remote regions with lower wind energy potential, such as central Alaska.

State and federal policymakers across the U.S. have noticed the potential of hydrokinetic energy, and have begun to support its development through legislative and mon-

etary means. Ocean energy is an eligible resource for credit under renewable electricity standards in sixteen states, in addition to federal renewable energy production tax credits, as expanded in the Energy Policy Act of 2005. Furthermore, hydrokinetic energy development was marked for increased research funding appropriations in the 2007 Energy Independence and Security Act. As of May 18, 2010, 143 preliminary permits have been granted by the Federal Energy Regulatory Commission (FERC,) allowing pilot projects development and technology impacts research around the nation (See the Figure 1.3).

Beyond the sheer size of the resource, hydrokinetic energy is attractive for its predictability. Wave patterns can be predicted days in advance, and tides for centuries. Since the kinetic energy held in a stream is related to its speed cubed, extracting the most electricity from each hydrokinetic project will depend heavily on site selection. A water current with double the speed contains eight times as much energy as one moving just half as fast. At this stage of the project, we focus mainly on in-stream-based hydrokinetic resources in design the oscillating hydrofoil, though we expect that the further modification to the oscillating hydrofoil will allow the device to harness energy from tidal or gulf streams as well.

2.2 Review of Hydrokinetic Technology

With the data of the hydrokinetic resources at hand, the relative performance of different types of hydrokinetic technologies in those different resources should be assessed as part of the requirements for any hydrokinetic project. It is hoped that such a comparison will provide information regarding the suitability of technology types to differing flow conditions encountered, with an end result of finding the optimum mechanism.

In this section, eleven in-stream hydrokinetic power generation project are surveyed. The technologies involved in those projects include traditional turbine systems, Vortex Induced Vibration, and a variety of fluid driven hydrofoil systems. The turbine is the dominant device used in the hydrokinetic power generation project, and it bears most of the hydrokinetic literatures; the Vortex Induced Vibration (VIV) mechanism is also explored as a method to extract hydrokinetic energy from tidal or in-stream flow. The VIV has long been proven to be a destructive engineering phenomenon and engineers have tried to suppress it until Dr. Michael Bernitsas suggested it be used for generating renewable electricity [17]. Other forms of hydrokinetic energy conversion technology, such as oscillating hydrofoils, have also been recognized [8, 9, 10, 15, 16]. Following these technology

summaries is a comprehensive survey of various hydrokinetic pilot projects reported to date in the public arena. Specific attention will be paid to the nontraditional hydrokinetic energy conversion schemes and the systems that are appropriate to be deployed in Alaska.

2.3 Assessment of Hydrokinetic Power Generation Projects

A number of resource quantifications and device demonstrations have been conducted throughout the world, it is believed that river flow and offshore ocean energy sectors will benefit from hydrokinetic technology. The project conducted and tested in Alaska also points out the fact that there are great opportunities for hydrokinetic energy exploration in the state of Alaska. In this section, five hydrokinetic power generator projects tested in Alaska will be introduced, then five non-turbine hydrokinetic power generation devices developed around world will be reviewed.

2.3.1 In-Stream Hydrokinetic Turbine at Ruby

The in-stream hydrokinetic turbine at Ruby [18], deployed by Yukon River Inter-Tribal Watershed Council (YRITWC), was Alaska's first hydrokinetic device to be connected to a local grid (Figure 2.1). It was also the first installed device anywhere in the United States near a river location. The turbine produced energy with no dams or water diversions. The turbine was floated on a pontoon boat and protected from interference introduced by the debris or floating logs by a debris boom. Even though the Ruby generator equipped with a 5 kW New Energy EnCurrent Turbine was only an experiment,it successfully showed the capability of producing enough power to support two households. This in-stream hydrokinetic turbine is a simple, scalable, and highly portable system which has the potential to be upgraded to supply power for a community or a larger district. The total project cost at Ruby is $65,000, which results in a higher cost per installed kilowatt than the current available power generated by diesel. This fact indicates that the hydro turbine was still a costly technology in Alaska at the time, which leaves some opportunities to improve or optimize.

2.3.2 Hydrokinetic Turbine Project at Eagle

The Yukon River hydrokinetic turbine project at Eagle [19] is an improved project based on the previously gained experience from the project at Ruby. The Eagle project was

Figure 2.1. Testing Ruby turbine project at Ruby, Alaska (Picture courtesy of ACEP)

proposed and advanced by the AP&T, who provides the Eagle residents with electricity. This hydrokinetic project is located just off the river bank at Eagle, Alaska, which is 171 miles northeast of Tok, Alaska, and approximately 8 miles down the river from the Alaska/Canada border. During the initial phase, the hydrokinetic turbine was suspended from a pontoon barge (Figure 2.2) to test its feasibility, and after one year the turbine system was moored to an anchor on the river bottom. It resembled a kite from an anchor in the riverbed. The turbine was modified to include an apparatus that allowed the turbine to operate in the river free of the barge. There was a substation located on the river bank to change the voltage from the turbine before it reaches the switch, or to act as a terrestrial anchor for the cable. AP&T claims that the turbine will remain in use from approximately May through September every year. The turbine system is hauled out before winter to protect it and perform maintenance, making diesel generation still necessary for winter.

The project currently is under a five year pilot phase. If the project proves feasible, a license for a 30-50 year deployment will be issued by the Federal Energy Regulation Commission (FERC) and additional units would be added to produce up to about 300 kW, to meet the whole area load. After that, the annual generation of the project is expected to be 1,000,000 kW, and the project will ultimately off-set the use of approximately 57,000 gallons of diesel fuel according to AP&T, which will save approximately $141,360 annually at 2008 prices. These savings will be passed on to the consumers by reducing their monthly charges depending on what percentage of hydrokinetic power is added to the local grid and the cost for a full size project. This result is a positive response to the AEA's recommendation that communities are encouraged to seek locally available resources and

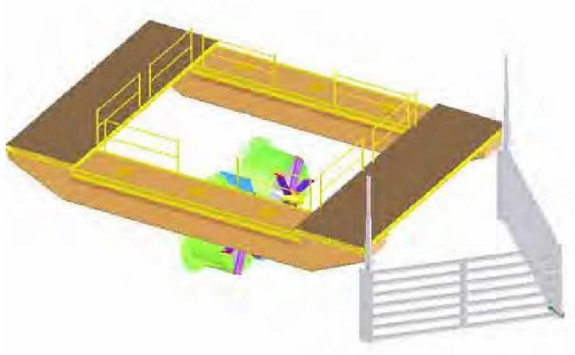

Figure 2.2. The practical implementation of the Eagle turbine

determine the most cost effective energy option for them.

2.3.3 The River In-Stream Energy Conversion (RISEC) Project at Igiugig

The project RISEC on Kvichak River by Igiugig Village Council [20] was developed by Electric Power Research Institute (EPRI) in Alaska to assess performance and economics of hydrokinetic devices in river location. Igiugig sits at the headwaters of the Kvichak River. Because it is located downriver from Lake Iliamna, in a relatively warm part of the state, Igiugig has much less summer/winter variability in flow. It makes Igiugig an excellent candidate for hydrokinetic power generation. A 40 kW project mounted on a 30 ft pontoon boat anchored to the riverbed was deployed. The 40 kW size of the project was based on low village energy consumption and resource availability during summer months. The pontoon boat was designed to serve as a platform from which four 4.5 ft turbine rotors could be suspended in the water column. There was also a protective "trash-rack" mounted in front of the rotors and generator to minimize debris impacts. Grid interconnection was accomplished using a short underwater cable from the units to the shore and connecting to the local grid via an existing distribution line. The cost for the 40 kW installation was about $300,000, with annual operation and maintenance at $12,000 per year. The total annual energy production was estimated at 200,000 kWh, which matched the summer load for Igiugig. The cost per installed kilowatt is about 65 cents, which is 33 cents lower than the 98 cents per kW the residents now pay for electricity.

Figure 2.3. The paddle wheel hydrokinetic device by Don Eller

2.3.4 The Paddle Wheel Hydrokinetic Project in the Tanana River

The paddle wheel hydrokinetic device was tested in the Tanana River by Mr. Don Eller [21] in November, 2009. It was a water surface mounted paddle wheel with partial blade submersion in the moving river stream and it utilized two gears with gear ratio of 80:1 for power transmission from the rotating wheel to a Permanent Magnetic Generator. Don Eller, who directed the project, claimed that the unit in (Figure 2.3) could produce 7-12 kW of power in a practical flow velocity of 4.5 meter per hour. More than 10 units are needed to produce all required electricity during the summer months for the community it was intended to serve. A simple comparison between the local diesel supply price and the system construction cost shows that diesel generation alone cost about $1040/month, whereas the paddle wheel hydrokinetic system only requests a single investment of $10,000 for construction. Once the paddle wheel is constructed, it will produce free energy until the next maintenance cycle. The potential to find an alternative to the diesel power generation makes this results attractive.

2.3.5 The Ocean Renewable Power Corporation TGU Projects

The Ocean Renewable Power Corporation (ORPC) is one of the most active clean energy companies devoted to harnessing hydrokinetic energy of the world's rivers and oceans. ORPC hydrokinetic power systems are mainly designed around their own proprietary Turbine Generator Unit (TGU), which is shown in Figure 2.4. The TGU turbine rotates in one direction only, regardless of current flow direction. Two cross flow turbines drive a

Figure 2.4. ORPC turbine generator unit

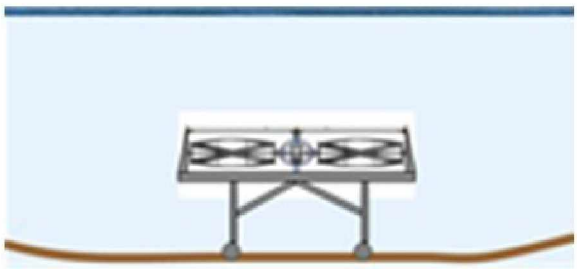

Figure 2.5. A single RivGen™ TGU and bottom support frame

permanent magnet generator on a single shaft. The TGU has a modular design that makes it easy to adapt to the varying needs of different site environments. TGUs can be stacked (horizontally or vertically) and incorporated into different scale modules that contain the mooring and power control system.

The RivGen™ Power System (Figure 2.5) by ORPC is specifically designed to generate electricity from small river sites. Arrays of TGUs are secured to the riverbed using bottom support frames as shown in Figure 2.5, The RivGen™ Power System is designed to connect directly into existing diesel-electrical grids, and to provide automatic fuel-switching so that whenever the RivGen™ Power System is generating power, the diesel generator automatically turns down or off. Depending on community needs and site size, the RivGen™ Power System can include up to several dozen TGUs, with each TGU generating up to 30 kW in a 3 m/s river current. ORPC is applying for a testing permit from FERC for a site on the Tanana River near town of Nenana at Alaska. To test the RivGen™ Power System, the project will seek to collect data on many vital questions for all kinds of hydrokinetic projects, including environmental interaction, performance and efficiency, deployment challenges, support design, debris avoidance, and energy economics. The TidGen™ (Figure 2.6) Power System by OPRC, designed to generate electrical power at water depth of 15 meters to 30 meters, is used at shallow tidal and deep river sites. In this system,

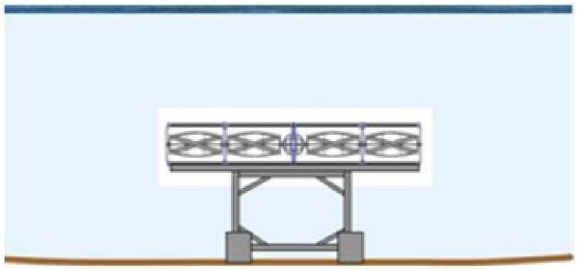

Figure 2.6. A single TidGen™ TGU and bottom support frame

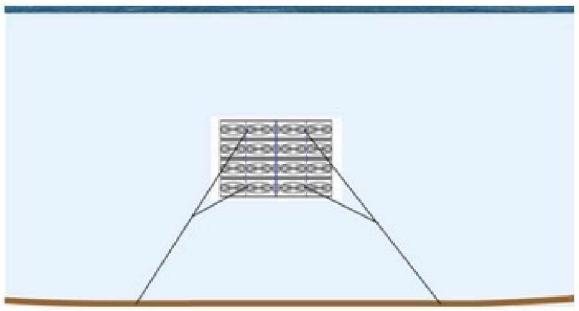

Figure 2.7. A single moored OCGen™ module made of four TGUs

groups of TGUs connect directly to an on-shore substation through a single underwater transmission line. The TidGen™ Power System is larger and more powerful than the RivGen™ Power System, with each TGU generating up to 250 kW in a 3 m/s water current.

The OCGen™ (Figure 2.7) Power System by OPRC is designed for use in water depths of more than 24 meters. Four TGUs are stacked together to create larger power generating capacity in OCGen™ Power System. The system is moored to the sea floor. Anywhere from a few to several dozen modules will be located at the same site, and will be connected in groups to an on-shore substation through a single underwater cable. A module composed of four TGUs will have a peak generating capacity of 1,000 kW in a 3 m/s water current.

2.3.6 Sea Snail Project

Sea Snail was a tidal energy project conceived and developed by researchers at Robert Gordon University, Scotland, UK. It was a horizontal axis turbine launched off the coast of Orkney in 2003 as a trial, and the full size version was installed at Burra Sound in Orkney in 2005. What made it stand out was the project's mounting strategy. The team

Figure 2.8. Sea Snail tidal energy converter

implemented reversible hydrofoils (See Figure 2.8) to produce a down force to keep the turbine in place. Given the fact that it is very difficult to attach something to the seabed or riverbed in areas of energetic flows, this project tried to establish a solution by deploying an innovative stabilizer in fast moving flows. The basic physics used in this project was very similar to the design in our project. The Sea Snail project made use of six water foils, and each foil was capable of pitch motion in order to adjust the lift force and the drag force in deployment process. When the device reaches the seabed, the foils are configured to be upturned, resulting in the maximum downward force so that the whole system can be held at the right position without slip. The turbine attached on the main frame will generate electrical power from the tidal flows. The experimental data shows that the water foil in the Sea Snail can operate with an average lift coefficient of 0.7 and drag coefficient of 0.18. This indicates the foil stabilizer can provide an amount of vertical force about 4 times that of the horizontal force, therefore guaranteeing the hydrokinetic system against slippage.

2.3.7 Stingray Tidal Stream Energy Project

Engineering Business Ltd. (now IHC Engineering Business Ltd.) started investigating the renewable energy market in 1997. Stingray was the first tidal stream energy project the company developed. Stingray (See Figure 2.9) used the flow of the tidal stream over a hydrofoil to create an oscillating motion that operated hydraulic cylinders to drive a electrical generator. This device is mounted on the seabed and is suitable in water depth

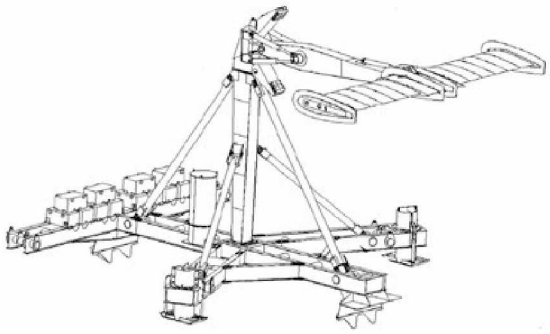

Figure 2.9. Stingray prototype

up to 100m. The project was divided into three phases to verify the design step by step. The first phase was a conceptual design. In September 2002, the second phase of the project installed a 180 ton, 150 kW machine near the Shetland Islands in the Highlands. The device was later removed safely with data collection for analysis and aid for future design and improvement The third phase of the project was a reinstallation of the demonstrator in the same spot as the second phase test in 2003. In the third phase, the device included a more flexible control system to allow the performance of the generator to be accurately controlled and experimental data was recorded over a long period of time. It achieved a mean hydraulic power of 85.4 kW in average current speed of 2 m/s over a 30 minutes period. The EB proposed future plans for the Stingray include a 5 MW pre-commercial Stingray farm to be connected to a local power distribution system in order to test whether the oscillating device is an economical technology for hydrokinetic power generation.

2.3.8 Oscillating Wing Hydropower Generation

The research on the oscillating wing hydropower generator [15, 16] was conducted by K.D. Jones and other team members at the Department of Aeronautics & Astronautics, Naval Postgraduate School, USA. They followed the classic work on a benchmark device called "windmill" by Mckinney and Delaurier to further develop the prototype of oscillating wing micro-hydropower generator. The principle used in the "windmill" was quite similar to the basic principle in our project in the way that a passive wing in dynamic flow will move in both pitch and heave degrees of freedom, if an airfoil is mechanically coupled in the pitch and heave, it can extract energy from the flow. K.D. Jones conducted computational modeling and experimental tests of tandem wings oscillating in a combined

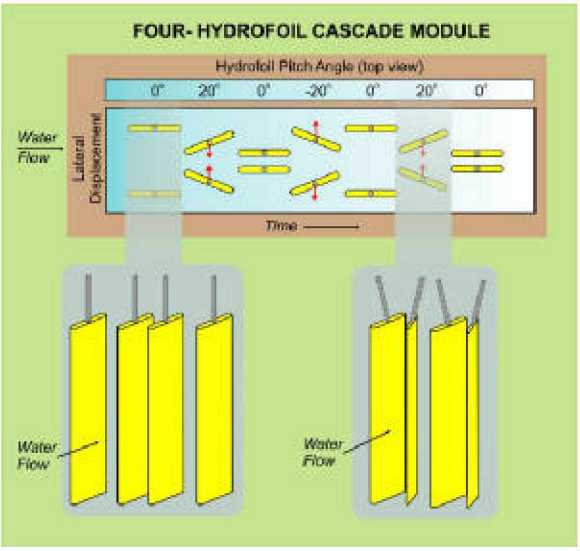

Figure 2.10. OCPS hydrokinetic device by Arnold Energy Systems (Courtesy of Arnold Energy Systems)

pitch-heave mode with approximately 90 degree phase angle between the two motions. Their experiment's results with Reynolds number equal to 2.2×10^4 digressed somewhat from the predictions of Navier-Stokes solved with a Reynolds number equal to 2.0×10^4. Their explanation about this inconsistency is neglecting of mechanical friction, mechanical mass, and buoyancy in the numerical simulation. Their research warns us that we should carefully simplify the conceptual design in order to obtain the accurate simulation result in the numerical modeling process. The quality of the simulation depends on how we set up the boundary condition and subdomain condition settings. To build an optimal model, the effects of mechanical friction, mechanical mass, and buoyancy should be accounted for.

2.3.9 The Oscillating Cascade Power System (OCPS)

The Oscillating Cascade Power System (OCPS) developed by Arnold Energy Systems [22] was based on a hydrodynamic phenomenon referred to as "flutter" to convert fluid kinetic energy into electrical power. The OCPS generator included a cascade of vertical hydrofoils submerged in moving water. This array of hydrofoils oscillates in anti-phase, (See Figure 2.10) at resonance (flutter) in a slow swimming motion, resulting in power transfer from flowing water to electricity. The official document claims that the system is capable of converting the oscillating mechanical energy into a steady electric current with an overall efficiency reaching 60%. One primary advantage of the system design is that it is highly

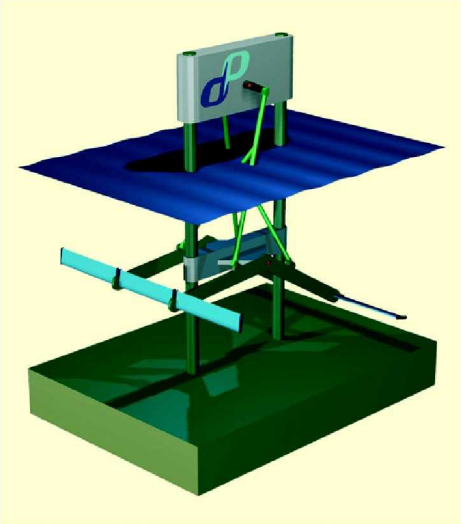

Figure 2.11. Pulse Stream 100 tidal energy converter (Courtesy of Pulse Tidal Ltd.)

scalable, from large utility power stations down to village-scale and even small stand-alone units. A typical medium scale OCPS of 50 m width and 12 m height operating at 60% efficiency in a water flow rate of 3 m/sec would produce approximately 4.9 MW. The Arnold Energy Systems claimed that the system, when it became a commercial production of modular units, could produce electric power at about sixty percent lower cost than traditional hydropower plants.

2.3.10 The Pulse Stream 100 Tidal Energy Converter

The Pulse Stream 100 is an offshore tidal energy converter developed by the UK company Pulse Tidal (Figure 2.11). The device implements two flat, foil type device to generate electric power from ocean tides. Specifically, two horizontal hydrofoils are configured to move up and down under tidal force. The length of the hydrofoils has no limitation due to its horizontal configuration instead of vertical deployment such as rotational turbine. By design, it also surpasses the turbine counterparts in that the Pulse Stream 100 is capable of extracting energy from relatively shallow waters close to shore, where it is needed, massively reducing the investment required to install, connect and maintain devices compared to those in remote locations. According to the company, the device can generate four times the power of competing "horizontal axis" machines in any given water depth. The team of engineers from Pulse Tidal installed the pilot device in Humber Estuary near Imming-

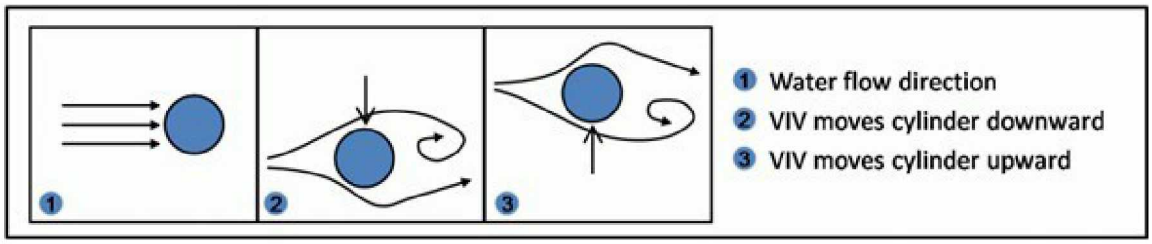

Figure 2.12. The illustration of Vortex induced Vibration

ham, UK. The project is the world's first grid connected shallow river tidal generator. The 100kW Humber prototype system uses tidal streams to oscillate horizontal blades. This mode of operation is the key to the device's unique access to shallow water and has so far shown that it can harness enough energy to power 70 homes. The project have been supported by a number of investors, including IT Power, Marubeni Europe plc, LIFE-IC and The Viking Fund, as well as by government grants. In the near future, Pulse Tidal will build a much larger device capable of providing about 1000 homes electricity. They are currently negotiating the location for the first full-scale project, which will begin operation in 2012.

2.3.11 Vortex-Induced Vibrations for Aquatic Clean Energy (VIVACE)

VIVACE uses Vortex Induced Vibrations (VIV) to extract energy from ocean, river, tidal and any other slow water current. The idea was invented by Professor Michael Bernitsas of the Department of Naval Architecture and Marine Engineering at the University of Michigan [17]. For decades, engineers have been trying to prevent the VIV phenomenon from damaging offshore structure. Professor Michael Bernitsas shifted the paradigm from suppressing the VIV to employing the VIV to harness energy from flowing water. As depicted in Figure 2.12, Vortex Induced Vibrations result from vortices forming and shedding on the downstream side of a bluff body in a current. Vortex shedding alternates from one side to the other, thereby creating a vibration or oscillation. The VIVACE is unlike any existing hydrokinetic technology, such as turbine, propellers, and foils. It converts the horizontal hydrokinetic energy of currents into a cylinder's vertical kinetic energy. The motions of the cylinder move a magnet up and down inside a metal coil, creating a DC current. In addition, the oscillations of the cylinder are rather slow with a speed of a cycle/sec, creating no threat to fish. Based on VIVACE technology, a company called Vortex Hydro Energy

LLC (VHE) was established in 2005. Their projects are funded by the U.S. Department of Energy and the Office of Naval Research and currently operated in the Marine Hydrodynamics Laboratory at the University of Michigan. Several successful laboratory tests by the team provided strong evidence to proceed to a multi-Kilowatt field demonstration. On August 2nd 2010, VHE conducted an open water test of its latest VIVACE converter. The device was tested in the St. Clair River at Port Huron, MI.

2.4 Further Remarks about the Reviewed Projects

Based on the literature reviews, the conversion schemes can be categorized in two broader classes: the turbine system and non-turbine system. For the category of turbine systems there are basically two different rotor types: vertical axis turbine and horizontal axis turbine. The vertical axis turbine is characterized by having the axis of rotation perpendicular to the flow. The horizontal axis turbine can be subclassified into two types: axial flow turbine and cross flow turbine. The rotational axis of the axial flow turbine is parallel to the incoming water stream; it is also called the propeller-type turbine. The rotational axis of cross flow turbine is parallel to the water surface but orthogonal to the incoming water stream. A cross flow turbine does not need to be oriented to the flow direction. It can also work in any depth of flow water.

However, a turbine can only harness a fraction of the available power in the free flowing water. A very popular model developed to describe the extractable power can be expressed as:

$$P = \frac{1}{2} C_p \rho V^3, \tag{2.1}$$

where ρ is the density of the water, A is the area swept by the turbine and V is the mean velocity of the flowing water. The turbine power coefficient, C_P, is the percentage of power that the turbine can extract from the current. The limit of 59% is usually assumed to be the theoretical upper limit for C_P. Due to low current velocities, the rotor of a river current turbine will experience low rotational speed. Standard generators are, in general, designed for a higher rotational speed. Thus, most river current turbine prototypes have been equipped with a gearbox between the rotor and the generator, but this will significantly increase the cost of the project and the complexity of the system design.

Besides the hydro turbine system, other non-turbine hydrokinetic conversion technologies have been designed to reduce the cost of the project, increase the capacity, and adapt to the exceptional hydro resources to generate electrical power. In general, the Stingray Tidal

Stream Power Generation System, Oscillation Wing Hydropower Generation System, the Oscillating Cascade Power System, and the Pulse Stream 100 Tidal Energy Converter utilize a hydrofoil to harness hydrokinetic energy. The Stingray project is a horizontal oscillating hydrofoil that has been tested in tidal current. In 2003, the Stingray Tidal Stream project demonstrated a mean output electrical power of 85.4 kW in average current speed of 2 m/s. However, the project was terminated because it had a very complex control system and was too expensive to manufacture and maintain. The core idea of Oscillation Wing Hydropower Generation system resembles the oscillating device we tested. The project is limited to laboratory tests and numerical simulations, and has never been constructed due to its complex control manipulation mechanism. The Pulse Stream 100 tidal energy converter has been successfully demonstrated and proved for the first time the potential for tidal stream energy from shallow waters. The VIVACE project makes use of the Vortex Induced Vibration by deploying cylinders in low speed water. Professor Michael Bernitsas and his students brought their research achievements out of the laboratory and built a business based on VIVACE technology. Their latest converter demonstration shows that the VIVACE can produce economic electrical power and have no observed negative impact on the environment or the fish in the river.

2.5 Summary

The device described in the following chapters is completely new compared to the above reviewed projects. What makes it stand out is that it is equipped with a simpler control scheme, which consumes less power to run the hydrofoil continuously in a oscillation manner. In the "Stingray" project, a hydraulic pump has been used to control the position of the foil and interface to the electric power generation system. The amount of energy consumed to control the "Stingray" hydrofoil is significant and degraded the system to such a degree that it was not applicable to generate economic electricity. The hydrofoil energy converter uses a low power micro-controller and linear actuator to control the orientation of a slender trim tab in water. The oscillating motion of the hydrofoil energy converter and the electricity power generator is coupled through an efficient linear to rotational motion conversion mechanism, called Scotch Yoke. The compact system architecture will make the power generation more efficient.

As with the most hydrofoil energy converters, the system is also highly scalable. The dimension of the system can be increased according to the water resource. Compared to

the scalability of the turbine system, the efficiency of our hydrofoil system will be dramatically increased when doubling the hydrofoil surface area, while the turbine's efficiency is limited by the length of the blade. With longer blades, the turbine will introduce more hazardous impact to the marine habitant and navigation.

Besides the higher energy density and the superior scalability of our system, our MHPG system has little chance of causing mortality due to its gentle motion. The hydrofoil in our device is generally oriented with the angle of attack less than 30 degree from the current, keeping debris build up at a minimum. Consequently, the build-up of debris on a conventional hydro turbine can easily disable or even destroy the turbine.

To sum up, our unprecedented design has the potential to solve many issues that the available technologies handle insufficiently, such as energy efficiency, debris attack, and marine habitant mortality, etc. The detailed study about the MHPG system will be presented and theoretical study about the fluid structure interaction will also be shown in next chapter.

Chapter 3
Oscillating Hydrofoil System and Modeling

Chapter 2 gives an overview of current hydrokinetic power generation technologies. This chapter will introduce the innovative design of oscillating hydrofoil in detail. The chapter is divided into five sections. In the first section, the core design of the oscillating hydrofoil is introduced. In the second section, the principal parameters of an oscillating hydrofoil are presented. In the third section, a brief introduction of hydrodynamic modeling using COMSOL Multiphysics is presented, then several COMSOL models are built and the modeling parameters are tabulated are tabulated. The simulation results and discussion about these results are also presented at the end of this section. In the fourth section, the hydrofoil motion generation system is studied as a trajectory planning robot arm using kinematics and dynamics in robotic control theory. In the fifth section, a Scotch Yoke mechanism is designed as the linear to rotational motion converter for the MHPG system.

3.1 The Concept of Hydrofoil Oscillator

Although many hydrokinetic energy conversion system have been proposed, most are facing licensing issues because of their negative impacts on the environment and their low energy and engineering efficiency. Due to the public concern about environmental problems and license request pressure, the California Energy Commission (CEC) [23] and the Department of Energy (DOE) of the United States [24] have defined general requirements that ocean and river energy conversion devices must satisfy to be considered for a license to operate in the United States. Those requirement are the following: (1) have high energy density, (2) not obstruct navigation, (3) not diminish the value of expensive coastal real estate, (4) be friendly to marine life and the environment, (5) have low maintenance, (6) be robust, (7) meet life cycle cost targets, and (8) have a minimum life of 10 - 20 years. The challenge of meeting all of these requirements has been the focus of more than 40 years of worldwide efforts — particularly in Europe and Japan and to a lesser extent in the United States [25, 26, 27]. Numerous devices have been designed and patented and several pilot devices have been launched [25, 28, 29]. However, a universally acceptable technology has not yet been developed [26, 27].

Generally, there are three sources of hydrokinetic energy: waves, in-stream currents, and tides. Some examples of how hydrokinetic energy converters fail to satisfy some of the CEC/DOE criteria are as follows.

- Wave energy converters based on surface oscillation, such as water column, buoy, flap, or pendulum [25, 26], have high energy output only in a very narrow band of wave frequencies near resonance. At any particular location, waves are random, allowing for a small window of optimal performance. In addition, waves occasionally apply extreme loads to structures.

- Converters of tidal current energy (turbines and watermills) can extract energy proportionally to their projected surface at an efficiency of 15 - 30 % and only for currents stronger that 2 m/s, below which they do not function efficiently [28].

- Tidal energy converters require at least a 5 m head, and are very large and as obtrusive as water dams. They also require a 5 - 7 year construction period and significant initial capital cost [28].

- Most of the converters operate on the surface and near shore and occupy valuable coastal real estate.

- Converters such as watermills, turbines, or tidal dams disturb marine life.

In view of the project reviews in chapter 2 and the case by case discussion, there remains a need in the hydrokinetic technology for a low-cost, in-stream system to utilize the energy in a fluid stream as an electrical generator. By design, our system meets most of the requirements by the CEC and the DOE of the United State: it does not obstruct navigation, does not diminish the value of expensive coastal real estate, and is friendly to marine habitant. The other requirements, such as having a low maintenance, being robust, meeting life cycle cost targets, and having a minimum life of 10 - 20 years, will be met by further design and optimization, since these requirements depend highly on the hardware implementation.

In a preferred embodiment, the oscillating hydrofoil system [14] provides a hydrodynamic power-generating system including a motion-generating subsystem disposed in a dynamic source of water such as a river. The motion-generating subsystem is retained in placed in the dynamic water source by a support subsystem and is connected to a power plant by a rod. The motion-generating subsystem is configured to oscillate and pivot under hydrodynamic force. The power plant is connected to the motion-generating subsystem to then convert the oscillating motion of the rod to electrical power.

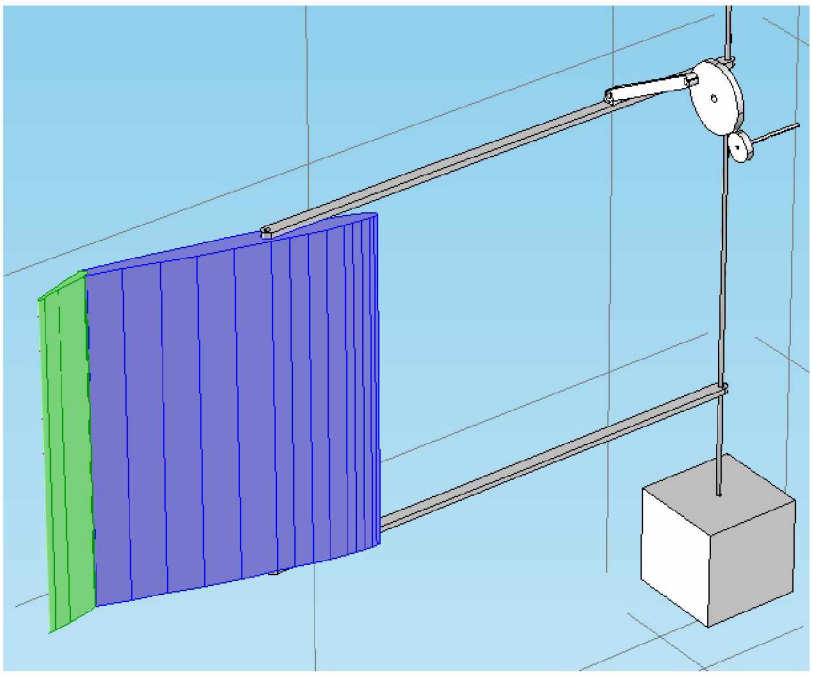

Figure 3.1. Three dimensional digital prototype of the hydrofoil system

Specifically, the motion-generating subsystem (Figure 3.1) includes a pair of spaced beams, which have upstream end and downstream end. The spaced beams are pivotally supported within the water at the upstream ends by the support subsystem. A pair of shafts are connected to and between the beams at the upstream ends and the downstream ends, respectively. The motion-generating subsystem includes a foil pivotally disposed between the downstream ends of the beams. The foil has an upstream edge and a downstream edge. A trim tab is pivotally disposed at the downstream edge of the foil. The trim tab may be actuated between a first position which causes the foil to pivot in one direction, and a second position which causes the foil to pivot in the opposite direction. The pivoting of the foil changes the direction of the hydrodynamic force acting on the hydrofoil, thus prompting the hydrofoil and the beams connected to it to oscillate back and forth.

The motion-generating subsystem is able to be deployed in flowing water resources such as rivers and estuaries, where the kinetic energy of the moving water can be harnessed as a energy source to generate electricity. With relatively few components, the motion-generating subsystem can be fabricated easily and inexpensively, thereby being readily available to those living in out-lying areas along waterways, where conventionally generated power may not be available.

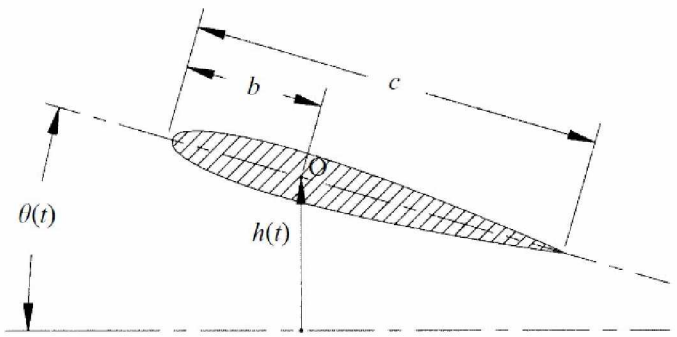

Figure 3.2. Definition of principal motion parameters for an oscillating foil

3.2 Principal Parameters of an Oscillating Foil

With the general idea about the oscillating hydrofoil introduced in the Chapter 1, let us consider a single hydrofoil, whose two dimensional diagram is shown in Figure 3.2 with chord length c. In fluid condition, the hydrofoil will perform a harmonic transverse (heave) motion, $h(t)$, of amplitude h_0 and frequency ω, and a harmonic angular (pitch) motion, $\theta(t)$, of amplitude θ_0 and frequency ω. The heave motion has a phase lead with respect to the pitch motion, which is denoted by ψ.

Under the interaction of the fluid and the hydrofoil, the hydrofoil is subject to time - varying forces $X(t)$ and $Y(t)$ in the x (forward) and y (transverse, or lift) directions respectively, and a torque $Q(t)$. The foil is assumed to pitch about a point O, whose distance from the leading edge is denoted by b. If T is the period of oscillation, we denote by F the time-averaged value of $Y(t)$, and by P the average input power per cycle, as:

$$F = \frac{1}{T}\int_0^T Y(t)dt, \tag{3.1}$$

$$P = \frac{1}{T}\left(\int_0^T X(t)\frac{da(t)}{dt}dt + \int_0^T Y(t)\frac{dh(t)}{dt}dt + \int_0^T Q(t)\frac{d\theta(t)}{dt}dt\right). \tag{3.2}$$

We define the power coefficient c_P as

$$c_P = \frac{P}{\frac{1}{2}\rho S_0 U^3}, \tag{3.3}$$

and the average transverse force, F, is non-dimensionalized as follows, to provide the thrust coefficient c_T:

$$c_T = \frac{F}{\frac{1}{2}\rho S_0 U^2}, \tag{3.4}$$

where ρ denotes the fluid density, and S_0 denotes the area of one side of the foil, i.e. for the rectangular foil used in this study, of chord c and span s, $S_0 = cs$. The energy harvest efficiency, η_P, is defined to be the ratio of useful power over input power, as

$$\eta_P = \frac{FU}{P}, \tag{3.5}$$

so that $\eta_P = \frac{c_T}{c_P}$.

There are five principal parameters in this problem, in addition to the shape of the foil (cross-section, aspect ratio):

1. The heave amplitude-to-chord ratio $h^* = \frac{h_0}{c}$;
2. The pitch amplitude θ_0;
3. The phase angle ψ between heave and pitch (heave leading pitch);
4. The parameter b^*, equal to the distance of the point about which the foil pitches from leading edge, b, divided by the chord length, i.e. $b^* = \frac{b}{c}$;
5. The non-dimensional frequency, called the Strouhal number St.

The strouhal number is a dimensionless value useful for analyzing oscillating unsteady fluid flow dynamics problems. it defined as

$$St = \frac{fA}{U}, \tag{3.6}$$

where f denotes the frequency of foil oscillation in Hz, i.e. $f = \omega/(2\pi)$, and A denote the characteristic width of the created jet flow. Since this is unknown before measurements are made, A is taken to be equal to double the heave amplitude, i.e. $A = 2h_0$.

Alternatively, we define a Strouhal number based on the total excursion (peak to peak) of the trailing edge of the foil, A_{TE}, when we will denote it by St_{TE}:

$$St_{TE} = \frac{fA_{TE}}{U}. \tag{3.7}$$

A importance derivative parameter to the performance of a foil is the maximum nominal angle of attack. If $\alpha(t)$ denotes the instantaneous angle of attack, referenced at the pivot point, then (Figure 3.3)

$$tan[\alpha(t) + \theta(t)] = \frac{1}{U}\frac{dh}{dt}(t). \tag{3.8}$$

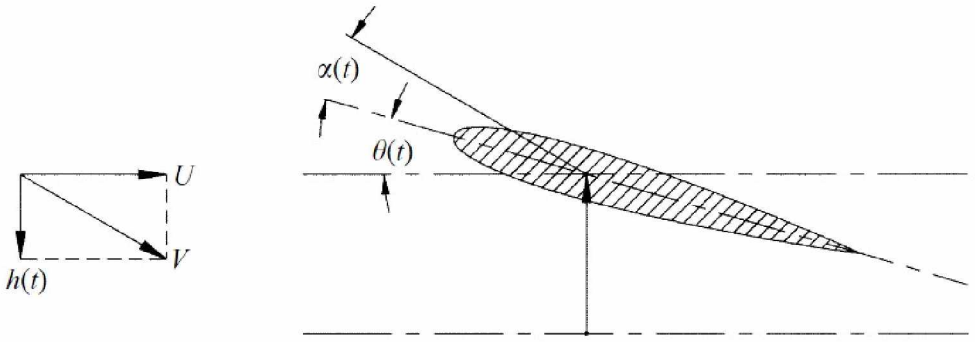

Figure 3.3. Definition of relative velocity V and nominal angle of attack $\alpha(t)$ for an oscillating foil

The maximum of $\alpha(t)$ must be determined numerically and will be denoted as α_{max}. An approximation for the maximum angle of attack, denoted as α_0, strictly valid only if the phase angle between heave and pitch is 90°, has been used primarily in the force measurement experiments, for simplicity:

$$\alpha_0 = arctan(\frac{\omega h_0}{U}) - \theta_0. \tag{3.9}$$

3.3 Hydrodynamic Modeling

Four areas of literature are relevant to the hydrodynamic modeling of an oscillating hydrofoil: oscillating foil for propulsion and maneuvering, airfoil modeling, fluid structure interaction, and hydrokinetic energy converters. The first three are very extensive and only a limited overview follows to define challenges in designing the hydrofoil used in hydrokinetic energy converter.

At the beginning of this section, the fluid force acting on the surface of the hydrofoil is analyzed. To that end, the interaction between the fluid and the structure is ignored, assuming a rigid hydrofoil positioned in the middle of free surface water channel. Following the equations for the fluid domain are introductions to four key parameters in numerical simulation, namely dynamic viscosity, Reynolds Number, lift coefficient and drag coefficient. At last, several COMSOL models are computed, further discussion about the simulation results presented at the end of this section.

3.3.1 Equations for the Fluid Domain

A two dimensional hydrofoil with chord length c is depicted in Figure 3.4. Suppose it surrounded by flowing water moving at constant forward speed u. Due to the fluid force,

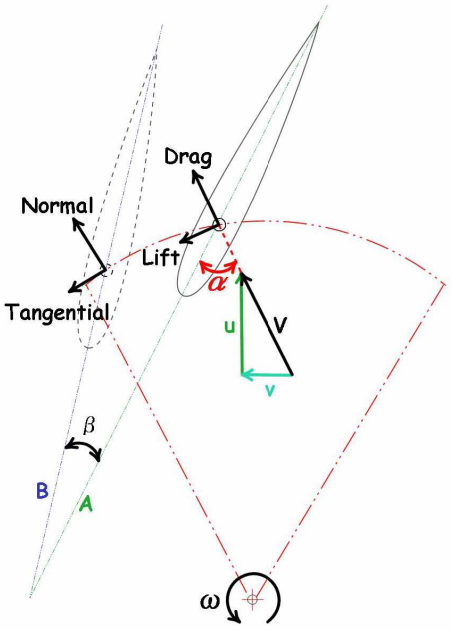

Figure 3.4. Diagram of fluid forces acting on a NACA0009 hydrofoil

the foil is subject to time varying lift force $L(t)$ and drag force $D(t)$, under which it will perform a harmonic transverse motion and a harmonic angular motion as we discussed in the previous section.

For the fluid, the basic equations are considered here to be the two laws of conservation for the physical system.

1. Conservation of mass (continuity)

$$\nabla \cdot \mathbf{V} = 0. \tag{3.10}$$

2. Conservation of momentum (Newton's second law)

$$\mathbf{F} = m\mathbf{a}. \tag{3.11}$$

For a fluid particle, it is convenient to divide Eq.(3.11) by the volume of the particle, so that it work with density instead of mass, as it is shown in Eq.(3.12)

$$\rho \frac{D\mathbf{V}}{Dt} = \rho\mathbf{g} + \mathbf{f}, \qquad in\ \Omega\ for\ t \in [0,T]. \tag{3.12}$$

Where $\rho\mathbf{g}$ is the applied body force per unit volume on the fluid particle, Ω is the domain occupied by the fluid at time t, $\mathbf{f}$ is the surface force which applied by external

stress on the sides of the element, for Newtonian fluid, it have

$$\mathbf{f} = \nabla \cdot \sigma, \tag{3.13}$$

in which σ is the total stress tensor:

$$\sigma = -p\mathbf{I} + \mu\left[\nabla\mathbf{V} + (\nabla\mathbf{V})^T\right]. \tag{3.14}$$

Combining Eq.(3.12), (3.13), and (3.14), the Navier-Stokes Equation for a Newtonian fluid consisting of pressure and viscous stress is given in Eq.(3.15)

$$\rho\frac{D\mathbf{V}}{Dt} = -\nabla p\mathbf{I} + \nabla\mu\left[\nabla\mathbf{V} + (\nabla\mathbf{V})^T\right] + \rho\mathbf{g}. \tag{3.15}$$

The velocity vector relationship of the water element near the surface of the foil is shown in Figure 3.4. Due to the relative movement of the foil and fluid, the current velocity u and the cross-stream foil velocity v are superimposed to yield the composed velocity V. It is the oncoming velocity the moving foil feels. From the perspective of velocity V, both the lift force and the drag force inserted by fluid flow can be determined because of Newton's second law. Further inspection will find that it is the tangential components of the lift force $L(t)$ and drag force $D(t)$ that are responsible for the transverse motion from position A to position B in Figure 3.4. Moreover, the applied torque will cause the foil to rotate around the central point O of foil when the foil is transporting. *Lift* is defined to be the component of surface force, which is exerted by a fluid passing by the surface of a body; *Lift* is perpendicular to the oncoming flow direction. It contrasts with the *drag* force, which is defined to be the component of the surface force parallel to the flow direction.

Based on the above analysis, the average force acting on the foil during the time when the rod moves from position A to position B can be calculated by

$$\overline{F} = \oint_S \left\{ \frac{1}{T_{A,B}} \int_0^{T_{A,B}} [L_T(t) + D_T(t)]\,dt \right\} dS. \tag{3.16}$$

The $L_T(t)$ and the $D_T(t)$ are the tangential components of the lift force and drag force, S is the contour of the foil in two dimensions and $T_{A,B}$ is the time span. COMSOL post processing can compute the reaction force of the water acting on the foil, thereby getting the total force at the downstream end of the rod.

3.3.2 Key Parameters in Numerical Simulation

This subsection briefly discusses four important parameters in fluid dynamic theory as the basis for COMSOL Multiphysics modeling. These parameters are dynamic viscosity,

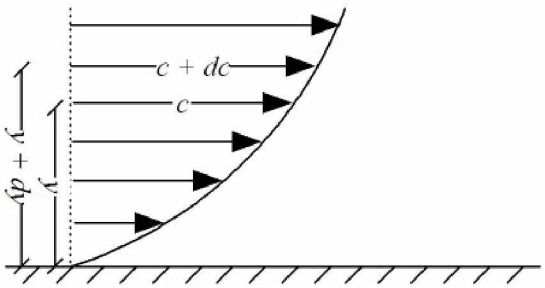

Figure 3.5. The shearing stress between the layers of non turbulent fluid

Reynolds number, lift coefficient, and drag coefficient. Dynamic viscosity is one of important parameters that affects the fluid motion near solid boundaries. Reynolds number is a key factor in determining what application mode should be used in COMSOL Multiphysics during simulation. Lift and drag coefficient is the evaluation metrics that used to quantify the capacity of the hydrofoil.

Dynamic (Absolute) Viscosity

The viscosity of a fluid is an important property in the analysis of liquid behavior and fluid motion near solid boundaries. The viscosity is the fluid resistance to shear and is a measure of the adhesive/cohesive or frictional fluid property. The resistance is caused by intermolecular friction exerted when layers of fluids attempt to slide by one another. Viscosity is a measure of a fluid's resistance to flow. Dynamic (absolute) Viscosity is the tangential force per unit area required to move one horizontal plane with respect to the other at unit velocity when maintained a unit distance apart by the fluid. The shearing stress between the layers of fluid moving in straight parallel lines can be defined for a Newtonian fluid as in the figure 3.5:

The dynamic or absolute viscosity can be expressed like:

$$T = \mu \frac{dc}{dy} \tag{3.17}$$

- T = Shearing stress
- μ = Dynamic viscosity

Reynolds Number

The Reynolds Number is a non dimensional parameter defined by the ratio of Dynamic pressure (ρu^2) and Shearing stress ($\mu u/L$) and can be expressed as

$$Re = \frac{\rho u^2}{\frac{\mu u}{L}} = \frac{\rho u L}{\mu} = \frac{uL}{v} \tag{3.18}$$

- Re = Reynolds Number (non-dimensional)
- ρ = Density (kg/m^3)
- u = Velocity (m/s)
- μ = Dynamic viscosity (Ns/m^2) (absolute)
- L = Characteristic length (m)
- v = Kinematic viscosity (m^2/s)

The Reynolds Number can be used to determine if the flow is laminar, transient or turbulent.

Lift and Drag Coefficient

The lift coefficient is a dimensionless coefficient that relates the lift force generated by a body, such as a wing or hydrofoil, to the dynamic pressure of the fluid flow around the body and a reference area associated with the body. It is also used to refer to the dynamic lift characteristics of a 2D airfoil section, whereby the reference "area" is taken as the foil chord. It may also be described as the ratio of lift pressure to dynamic pressure.

The drag coefficient is also a dimensionless quantity that is used to quantify the drag or resistance of an object in a fluid environment such as air or water. It is used in the drag equation, where a lower drag coefficient indicates the object will have less aerodynamic or hydrodynamic drag. The drag coefficient is always associated with a particular surface area. The drag coefficient of any object comprises the effects of the two basic contributors to fluid dynamic drag: skin friction and form drag. The drag coefficient of a lifting airfoil or hydrofoil also includes the effects of lift-induced drag. The drag coefficient of a complete structure such as an aircraft also includes the effects of interference drag.

The drag and lift forces themselves are not as interesting as the dimensionless drag and lift coefficients. Those coefficients depend only on the Reynolds number and the object's dimension. The coefficients are defined as:

$$C_D = \frac{2F_D}{\rho U_{mean}^2 D} \tag{3.19}$$

$$C_L = \frac{2F_L}{\rho U_{mean}^2 D} \tag{3.20}$$

- F_D and F_L are the drag and lift forces
- ρ is the fluid's density
- U_{mean} is the mean velocity
- D is the characteristic length, in this case the chord length of the hydrofoil

3.3.3 Hydrodynamic Modeling of the Oscillating Hydrofoil Mechanism

COMSOL CFD Module is an optional add-on package for COMSOL Multiphysics designed to solve and model Computational Fluid Dynamics (CFD), which is an increasingly important tool for modeling fluid-flow. We will use COMSOL CFD Module to simulate a turbulent channel and a hydrofoil inside the channel to study the interactive process between the fluid and solid mechanics. There are several fluid-flow physics interfaces available within the CFD Module of COMSOL Multiphysics. The various types of momentum transport that we can simulate includes laminar and turbulent flow, Newtonian and non-Newtonian flow, isothermal and non-isothermal flow, multiphase flow, and flow in porous media. How to chose the fluid-flow physics interfaces depends on the property of the particular application. Because our model is essentially a Newtonian flow problem, thereby either laminar flow interface or turbulent flow interface could be selected depending on the Reynolds Number. In our model, the Reynolds Number can be calculated as:

$$Re = \frac{\rho u L}{\mu} = \frac{1000(kg/m^3) \times 1(m/s) \times 0.09(m)}{0.001(Ns/m^2)} = 90000, \tag{3.21}$$

where the fluid velocity assumed to be 1 m/s.

Because the practical Reynolds Number calculated above is approaching 100000, and the flap's effects on the flowing water can create turbulent. Turbulent model can be used

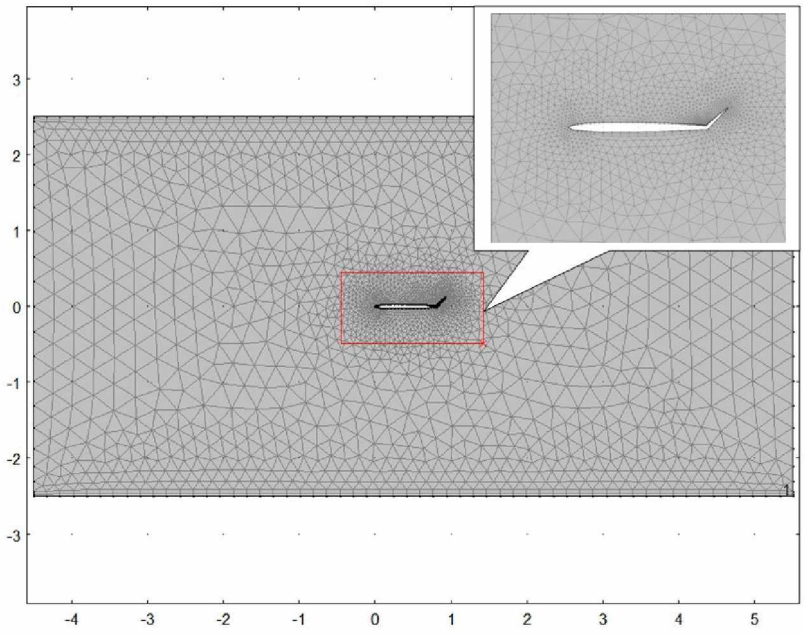

Figure 3.6. Meshed geometry

in COMSOL simulation. Turbulent Flow, k-ε Interface has been used in our modeling process. The interface has the equations, boundary conditions, and volume forces for modeling turbulent flow using the Reynolds averaged Navier-Stokes (RANS) equations, solving for the mean velocity field and pressure, and the k-ε model, solving for the turbulent kinetic energy k and the rate of dissipation of turbulent kinetic energy ε.

Figure 3.6 is the meshed geometry which was used to represent the 2D oscillating hydrofoil. Note the main body and the trim tap of the hydrofoil was simulated as a whole body in order to save computational expenses. The mesh technique used in the simulation is Physics - Controlled meshing, which is adapted to the current physics settings before compute the results. For example, for a fluid-flow model, a finer mesh can be automatically generated with a boundary layer mesh along the no-slip boundary settings. If the physics settings in the model have been changed and the meshing sequence rebuilt, it creates a new mesh adapted to the new physics settings. COMSOL has a variety of meshing techniques that can be explored depending on the specific application. For example, other available meshing methods include user-controlled meshes, structure meshes, unstructured meshes, ALE moving meshes [30].

Figure 3.7 presents the simulation result with COMSOL settings tabulated in Table 3.1. This model is the first successfully solved COMSOL model simulating the hydrofoil in a

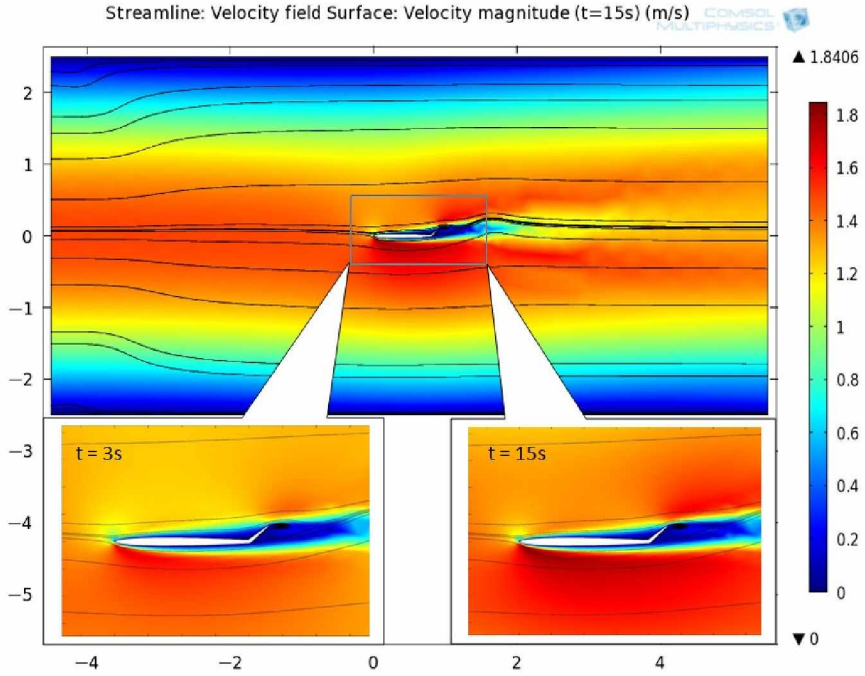

Figure 3.7. COMSOL solved result for 15 second fluid flow development

"in-stream river channel". From the two different time captures of the velocity distribution, the difference of the velocity magnitude around the foil can be observed. The fluid has fully developed in three seconds and continuously increased the velocity magnitude in the hydrofoil boundary layer area. Due to the fluid structure interaction, some streamlines passing by the hydrofoil reach the highest velocity of 1.8 m/s.

Based on the results of the above solved model, the lift force and drag force can be obtained from the COMSOL postprocessing procedure. The force on the hydrofoil can be examined in terms of the pressure differences above and below the hydrofoil, which can be related to velocity changes by Bernoulli's principle. The total lift force is the integral of vertical pressure forces over the entire wetted surface area of the hydrofoil:

$$L = \oint p\mathbf{n} \cdot \mathbf{k} dA, \tag{3.22}$$

- L is the lift
- A is the foil surface area
- p is the value of the pressure
- $\mathbf{n}$ is the normal unit vector pointing into the foil,

Table 3.1. Summary of COMSOL settings

1	COMSOL Version	4.1.0.88
2	Physics Mode	Turbulent, (k, ε)
3	Mesh Setting	Free Triangular
4	Maximum Element size	0.03
5	Study type	Time Dependent t = (0,0.2,20)
6	Time Stepping Method	Backward Differentiation Methods (BDF)
7	Steps Taken by Solver	Free
8	Maximum BDF Order	2
9	Minimum BDF order	1

- **k** is the vertical unit vector, normal to the free stream direction

The above lift equation neglects the skin friction forces, which typically have a negligible contribution to the lift compared to the pressure forces. COMSOL Multiphysics implement this integration as a black box function *reacf ()*. Applying the *reacf ()* operator on the dependent variable when doing a surface integration will get the force correspondence to the dependent varible. For example, in computational dynamics, with dependent variable u and v corresponding to $x-$ and $y-$ direction force, respectively.

In the next step, COMSOL will be used to answer the first important question about the capability of the oscillation hydrofoil that interests us. How much force can it generate to drive the electric power generator? To answer this question, the lift and drag force dependence on the angle of attack and time should be thoroughly studied. Ideally, if the results can be solved by directly setting up a compound time dependent model that include the hydrofoil dynamics, the answer to the question is obvious. However, due to the complexity of the hydrofoil application and the limitation of the COSMOL Multiphysics in solving this model, COMSOL is unable to completely solve this complex hydrofoil dynamics problem. Further study reveals that the hydrofoil will change its angle of attack while translating. It is proven that the magnitude of fluid force will change in accordance with the different angle of attack. To make the problem solvable, we will compute the necessary data individually; that is, to study the lift and drag coefficient in several separate models when the angle of attack is adjusted manually. Specifically, several similar models will be solved, in which the only difference is the angle of attack. In this case, the lift and

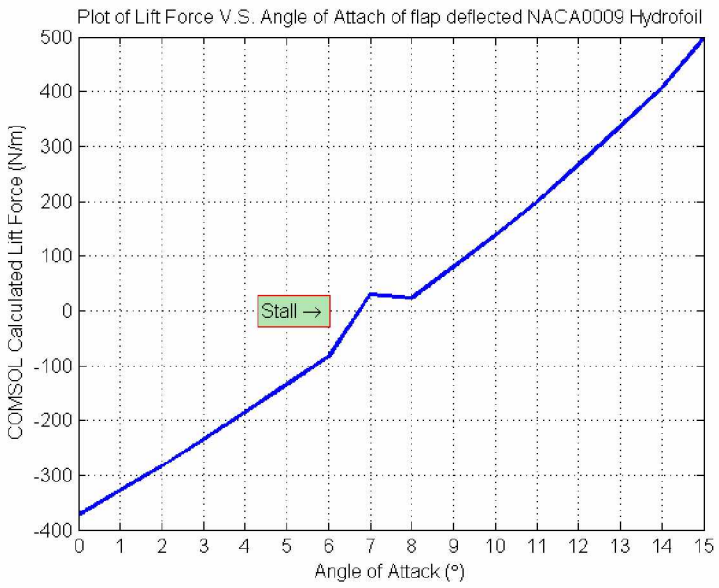

Figure 3.8. Plot of lift force V.S. Angle of Attack of flap deflected NACA0009 Hydrofoil

drag coefficients are solved and plotted separately. Given all of the lift coefficients under different angles of attack, the lift force V.S. angle of attack obtained from multiple models is shown in Figure 3.8. Please note here the fluid force is plotted to show the power of the oscillating hydrofoil.

In the process of getting these results, a very interesting phenomena is observed. It showed that vortices developed near the deflected flap affect the lift coefficient. With a certain angle of attack, the vortex created at the trailing edge was suppressed and the lift coefficient was significantly reduced. This effect was obvious when the angle of attack of the deflected hydrofoil is equal to 7°. This means when the angle of attack is equal to 7°, the hydrofoil will stall. This is also where the trim tab should switch to the other position in order to continuously generate oscillating motion. Figure 3.9 shows the lift coefficient of the hydrofoil when the angle of attack is equal to 7° and Figure 3.10 is the streamline plot of the model. From Figure 3.9, we can see the lift approximate zero when the flow has fully developed around the foil.

In summary, the motion of the hydrofoil in the model should comply with both the theories of fluid dynamics and manipulator dynamics. In the future, the fluid torque acting on the foil can be calculated using the Navier-Stokes Equation by COMSOL Multiphysics. The calculated force and torque can then be applied to the solid mechanics model. The

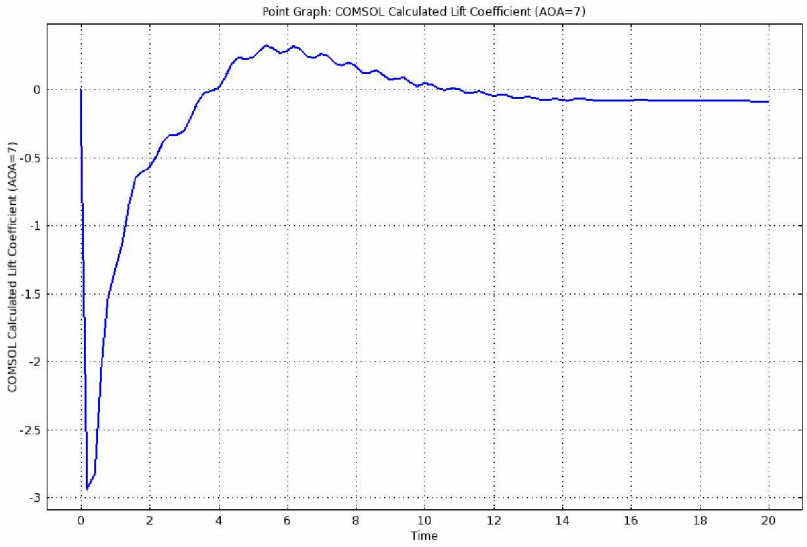

Figure 3.9. COMSOL calculated lift coefficient (Angle of Attack = 7°)

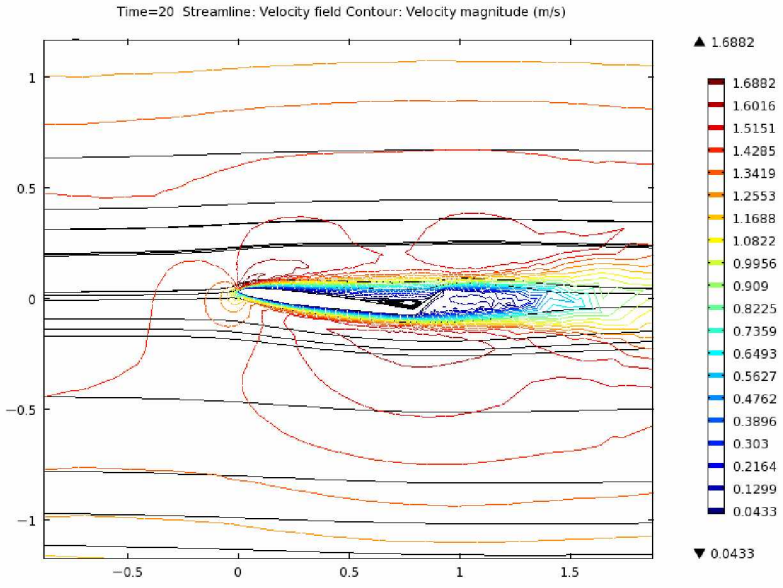

Figure 3.10. The Streamline and contour plot of the solution, (Angle of Attack = 7°)

ultimate model should solve all the problems in regard to the dynamics of the hydrofoil motion generation system. For example, the position of the beam, the orientation of the hydrofoil, and the velocity and the acceleration of the link components. The abstracted links's motion can then be solved explicitly by interfacing different software from different areas. In the next section, studying the hydrofoil with robotic trajectory planning theories will be presented and an evaluation of this methodology will be discussed.

3.4 Study of the Foil System as a Trajectory Planning Robot

Compared to a trajectory planning robot arm, the operation of oscillating hydrofoil resembles a robotic manipulator with few differences [31] (Figure 3.11). A robotic manipulator may be thought as a set of bodies connected in a chain by revolving joints. The hydrofoil system, the trim tab, the main body of the foil, and the support beam are equivalent to the links in a three-link planar arm, which is sometimes called the **RRR** mechanism. In robotic design, the links are numbered starting from the immobile base of the arm, which might be called link 0. The first moving body is link 1, and so on, out to the free end of the arm, which is link n. We can employ this notation in our hydrofoil system study. For example, the support beam is the link 1, the main body of the hydrofoil is link 2, the trim tab in the hydrofoil is the link 3. In this section we will study the hydrofoil with the theory of manipulator kinematics and dynamics.

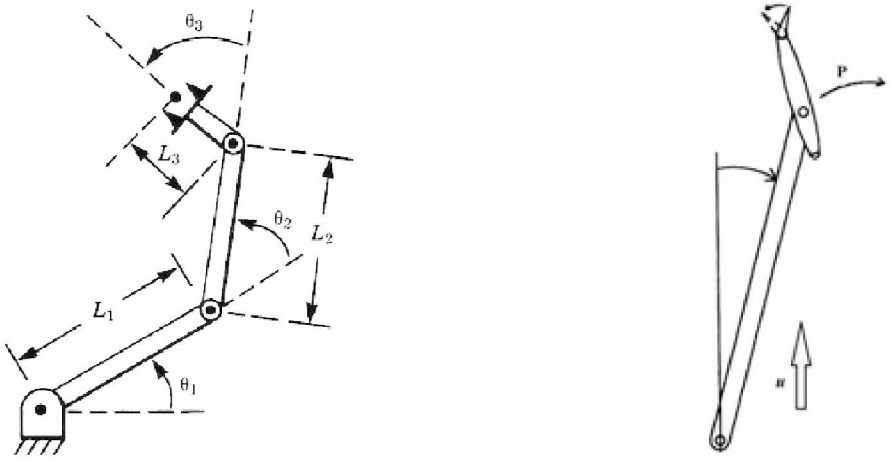

(a) (b)

Figure 3.11. (a) Three-link planar robotic arm. (b) The motion generating subsystem of the HPGS

3.4.1 Kinematics for Hydrofoil Trajectory Planning

The study of the hydrofoil kinematics refers to the geometrical and time-based properties of the motions. The relationship between these motions and the forces and torques that cause them constitutes the problem of dynamics, which will be discussed later.

A single link of the hydrofoil system has many attributes that need to be considered by the mechanical designer: the type of material used, the stiffness of the link, the location of the joint bearings, the external shape, the weight and inertia, etc.. The problem of connecting the links of a robot together is also raises many questions for the mechanical designer to resolve. However, for the purposes of obtaining the kinematic equation of the oscillating hydrofoil, a link in the hydrofoil is considered only as a rigid body that defines the relationship between two neighboring joint axes. Joint axes are defined by lines in space.

In order to describe the location of each link relative to its neighbors, frames attached to each link are defined. The link frames are numbered according to the link to which they are attached. That is frame $\{i\}$ is attached rigidly to link i. According to the convention denoted in [31] to locate the frame on the link, the link parameters in terms of the link frames are summarized as following:

- a_i = the distance from $\hat{Z}_i$ to $\hat{Z}_{i+1}$ measured along $\hat{X}_i$;
- α_i = the angle from $\hat{Z}_i$ to $\hat{Z}_{i+1}$ measured about $\hat{X}_i$;
- d_i = the distance from $\hat{X}_{i-1}$ to $\hat{X}_i$ measured along $\hat{Z}_i$; and
- θ_i = the angle from $\hat{X}_{i-1}$ to $\hat{X}_i$ measured about $\hat{Z}_i$.

In which $a_i > 0$, because it corresponds to a distance; however, α_i, d_i, and θ_i are signed quantities. These link parameters and their specific notation are the basics for deriving the dynamic equation of the system, which will be presented in the next section.

3.4.2 Dynamics of Trajectory Prediction of the Hydrofoil System (Forward Dynamics)

Manipulator dynamics is the study of the torques and forces that are required to cause the motion of the hydrofoil and the beam supporting it in the oscillating motion generating system. In this subsection, we will consider the equation of motion for an oscillating hydrofoil system. The equation of motion describes the interdependence between the motion and the torques applied by the actuators or from external forces. In our case, the hydrofoil

is driven by flowing water. The energy harnessing process takes place when the fluid force produces output power through the trajectory alternating of the hydrofoil.

There are two problems related to the dynamics of the oscillation hydrofoil, and both of them can be studied to solve the problems with which we are concerned. The first problem is to find the required vector of joint torques and external forces by the given trajectory displacement, velocity and the acceleration. From this perspective, we can investigate the energy efficiency of the oscillating hydrofoil. The second problem is to decide how the mechanism will move under application of a set of joint torques and forces. This method is useful to simulate the manipulator. Specifically, the joint torques and forces can be obtained by the COMSOL model. It was found and demonstrated that the fluid will insert a variable torque on the oscillating hydrofoil. The fluid torques and forces are equivalent to the joint torques and forces in the equation of motion of robot manipulator dynamics. The fluid force plays the role of the external force in a typical manipulator dynamics problem. The dynamic problem of the hydrofoil can be solved using the iterative Newton-Euler dynamics algorithm.

The Newton-Euler algorithm for computing joint torques from the motion of the joints is composed of two parts. First, link velocities and accelerations are iteratively computed from link 1 out to link n (Using the Equation 3.23, 3.24, 3.25, and 3.26) and the Newton-Euler equations are applied to each link (Equation 3.27 and 3.28). Second, forces and torques of interaction and joint actuator torques are computed recursively from link n back to link 1 (using equations 3.29 and 3.30),

$$ {}^{i+1}\omega_{i+1} = {}^{i+1}_{i}R\,{}^{i}\omega_i + \dot{\theta}_{i+1}\,{}^{i+1}\hat{Z}_{i+1}, \tag{3.23} $$

$$ {}^{i+1}\dot{\omega}_{i+1} = {}^{i+1}_{i}R\,{}^{i}\dot{\omega}_i + {}^{i+1}_{i}R\,{}^{i}\omega_i \times \dot{\theta}_{i+1}\,{}^{i+1}\hat{Z}_{i+1} + \ddot{\theta}_{i+1}\,{}^{i+1}\hat{Z}_{i+1}, \tag{3.24} $$

$$ {}^{i+1}\dot{v}_{i+1} = {}^{i+1}_{i}R({}^{i}\dot{\omega} \times {}^{i}P_{i+1} + {}^{i}\omega_i \times ({}^{i}\omega_i \times {}^{i}P_{i+1}) + {}^{i}\dot{v}_i), \tag{3.25} $$

$$ {}^{i+1}\dot{v}_{C_{i+1}} = {}^{i+1}\dot{\omega}_{i+1} \times {}^{i+1}P_{C_{i+1}} + {}^{i+1}\dot{\omega}_{i+1} \times {}^{i+1}P_{C_{i+1}} + {}^{i+1}\omega_{i+1} \times ({}^{i+1}\omega_{i+1} \times {}^{i+1}P_{C_{i+1}}) + {}^{i+1}\dot{v}_{i+1}, \tag{3.26} $$

$$ {}^{i+1}F_{i+1} = m_{i+1}\,{}^{i+1}\dot{v}_{C_{i+1}}, \tag{3.27} $$

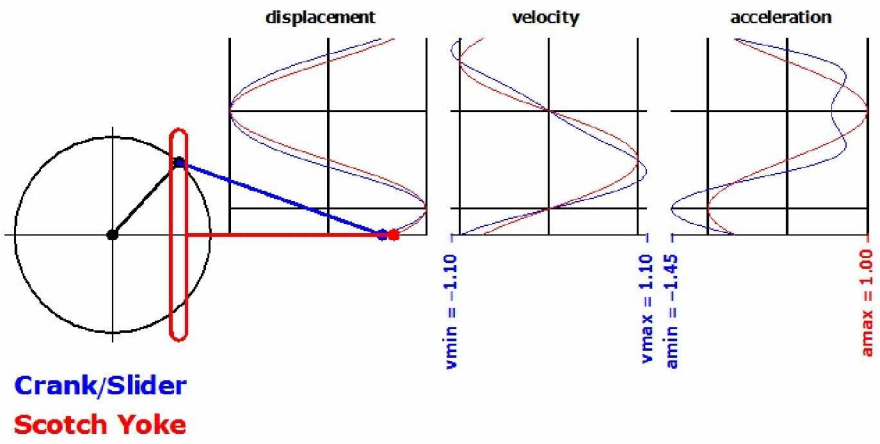

Figure 3.12. Comparison of Scotch Yoke and Crank Slider

$$ {}^{i+1}N_{i+1} = {}^{C_{i+1}}I_{i+1}\,{}^{i+1}\dot{\omega}_{i+1} + {}^{i+1}\omega_{i+1} \times {}^{C_{i+1}}I_{i+1}\,{}^{i+1}\omega_{i+1}. \tag{3.28} $$

$$ {}^{i}f_i = {}^{i}_{i+1}R\,{}^{i+1}f_{i+1} + {}^{i}F_i, \tag{3.29} $$

$$ {}^{i}n_i = {}^{i}N_i + {}^{i}_{i+1}R\,{}^{i+1}n_{i+1} + {}^{i}P_{C_i} \times {}^{i}F_i + {}^{i}P_{i+1} \times {}^{i}_{i+1}R\,{}^{i+1}f_{i+1}, \tag{3.30} $$

$$ \tau_i = {}^{i}n_i^T\,{}^{i}\hat{Z}_i. \tag{3.31} $$

These equations are summarized from [31] and are the substantial part of the algorithms used to compute the solution in Matlab.

3.5 Linear-Rotational Motion Conversion System Design

Crank mechanisms and Scotch Yoke have been employed in converting linear motion into rotational motion in our oscillating hydrofoil system, so as to be further coupled with a permanent magnetic generator. In the prototype design, the Scotch Yoke was selected because it has fewer moving parts and a smoother operation. From the comparison of two candidates of linear to rotational motion conversion mechanism, the Crank Slider and Scotch Yoke (Figure 3.12), similar displacement and velocity of the two mechanisms are observed. However, for the acceleration, the two mechanisms are quite different. The acceleration of the crank slider is fluctuated when the displacement is near the maximum

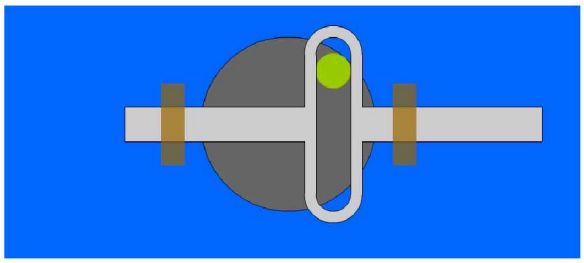

Figure 3.13. Scotch Yoke

point. The fluctuation increases the possibility of creating a dead point and the possibility of being worn out in the course of motion. Moreover, for a constant crank rotational speed of ω radians per second, the Scotch Yoke produces a displacement at time t of $cos(\omega t)$, a velocity of $-\omega sin(\omega t)$, and an acceleration of $-\omega^2 cos(\omega t)$. The plots in Figure 3.12 are normalized to these values, independent of any manipulated value of the crank angle. The displacement strip chart shows the relatively longer dwell time produced by the Scotch Yoke at the top of the stroke. Because a higher percentage of the time spent at top dead center improves engine efficiency, this feature is offered as a potential advantage in the design of linear-to-rotational motion conversion system.

The implementation of a Scotch Yoke includes a sliding bar, a yoke on that bar with a slot cut out, and a smaller bar connected to the yoke and affixed by a pin through the yoke slot to the sliding bar. As the bar slides back and forth, or reciprocates, the smaller bar is forced to slide up and down in the yoke slot, creating a rotational movement (Figure 3.13).

3.6 Summary

This chapter presented the core concept of the oscillating hydrofoil power generation mechanism. Several principle parameters for the oscillating foil were developed. These parameters can be used to evaluate or improve the performance of the system, or can be used as metrics when the oscillating foil is compared to other similar technologies. The hydrodynamic modeling section introduced the COMSOL Multiphysic software and briefly explained the basics of the COMSOL modeling process. Following the introduction to COMSOL is the derivation of equations for fluid domain and fluid force integration. These equations are necessary in solving the model in COMSOL. By setting up several different models in COMSOL, the results of applied fluid force of 500 N in a 15° Angle of Attack scenario and 7° stalling Angle of Attack were obtained.

The next section introduces the methodology of studying the oscillating hydrofoil as a trajectory planning robot. The closed form of the Newton - Euler dynamics algorithm can be used to solve the displacement, velocity, and acceleration of both the hydrofoil and the support rod.

In the last section, a Scotch Yoke mechanism was proposed to undertake the linear to rotational motion conversion for generating rotational motion to drive a rotor. The comparison between a crank slider and a Scotch Yoke showed that Scotch Yoke is a better choice for the oscillating hydrofoil system. Important parameters for designing the Scotch Yoke system were also presented in this section.

Chapter 4
Electrical Power Systems

In this chapter, a typical electric generator will be introduced. Synchronous generators, asynchronous generators, and linear configuration electric generators are compared in the aspects of requirement for the oscillating hydrofoil power generation system. Following the section about generators is a discussion about three configurations of micro-hydro power plant architecture, such as the Fixed-Speed Induction Generator(FSIG) configuration, Doubly Fed Induction Generator (DFIG) configuration, and Fully Rated Converter(FRC) configuration. The theoretical and conceptual details of those different configurations are discussed. Advantages and disadvantages of these three configurations are also presented to show that DFIG configuration is the best architecture to be deployed in the oscillating hydrofoil system.

4.1 Electric Generator

The electric generator is a device that converts mechanical power into electrical power. It basically forces electrons to flow through an external electrical circuit by moving a conductor through a magnetic field, thereby inducing an electrical voltage in the conductor. According to the characteristics of the output electric current, electric generators can be classified into two types: AC generators and DC generators. An AC generator converts mechanical energy into alternating current electrical power. There are two types of AC generators: asynchronous or induction generators and synchronous generators. The basic principle of those two AC generators will be discussed in this section. A DC generator, which uses almost the same electrical principles as an AC generator, produces a direct current electricity from mechanical energy by employing a commutator on the rotating shaft. It is this commutator that converts the alternating current produced by the armature to direct current. Besides those rotating electric generators, a linear generator draws much attention in the research community nowadays, because it is especially fit for those applications that make use of mechanical power from a piston engine or reciprocal motion.

4.1.1 Synchronous Generator

A synchronous generator consists of two elements: the field and the armature [32] (Figure 4.1). Because the power transferred into the field circuit is much less than the power transferred into the armature circuit, AC generators nearly always have the field wind-

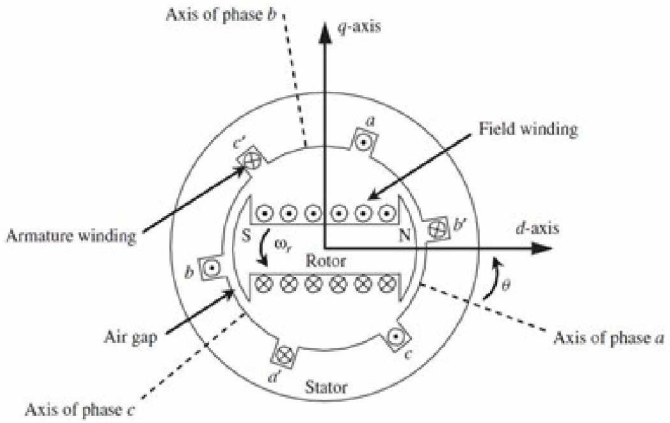

Figure 4.1. Schematic diagram of a three-phase synchronous generator

ing on the rotor and the armature winding on the stator. The armature consists of many winding wires connected in series or parallel to obtain the desired terminal voltage. The armature winding is placed into a slotted laminated steel core. A synchronous machine also consists of a revolving DC field - the rotor. A mutual flux developed across the air gap between the rotor and stator causes the interaction necessary to produce an EMF. As the magnetic flux developed by the DC field poles crosses the air gap of the stator windings, a sinusoidal voltage is developed at the generator output terminals. This process is called electromagnetic induction.

Synchronous generators are used because they offer precise control of voltage, frequency, VARs and WATTs. This control is achieved through the use of voltage regulators and governors. If electromagnetic excitation were applied, the magnitude of the AC voltage generated is controlled by the amount of DC–exciting current supplied to the field. If permanent magnetic excitation were applied, the voltage magnitude would be controlled by the speed of the rotor ($E = 4.44fnBA$). However, this would necessitate a changing frequency in the MHPG system. Since the frequency component of the power system is to be held constant, solid state voltage regulators or static exciters are commonly used to control the field current and thereby accurately control generator terminal voltage. The frequency of the voltage developed by the generator depends on the speed of the rotor and the number of field poles. For example, the output frequency of a 60 Hz system is equal to $speed(\mathbf{rpm}) \times polepairs/60$.

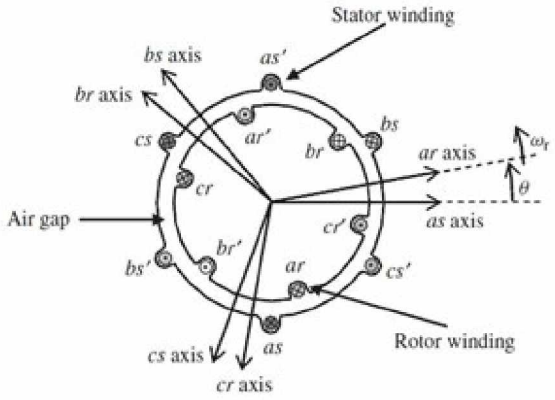

Figure 4.2. Schematic diagram of a three-phase asynchronous generator

4.1.2 Asynchronous (Induction) Generator

A second type of AC generator is the asynchronous generator [32], or induction generator. Although the induction motor is the most common of all motors, it is seldom used as a generator before it has been found to be well-suited for wind power applications in recent years. It is more flexible in variable speed control of a wind turbine and can be used as a frequency changer. Like the synchronous generator, the stator winding of an induction generator is excited with alternating currents. In contrast to a synchronous generator in which a field winding on the rotor is excited with DC current, alternating currents flow in the rotor windings of an induction generator. Rotor currents are then produced by induction, i.e., transformer action. The induction machine may be regarded as a generalized transformer in which electric power is generated between rotor and stator together with a change of frequency due to an inflow of mechanical power.

In the induction motor, the stator windings rotor winding are essentially the same as those of a synchronous machine. However, the rotor windings do not just develop a magnetic field between the air gap; the rotor and the stator field are coupled by a transformer action through the air gap. As in a synchronous generator, the armature flux in the induction generator leads that of the rotor and produces an electromechanical torque. In fact, we will see later in this chapter that the rotor and stator fluxes rotate in synchrony with each other and that torque is related to the relative displacement between them. However, unlike a synchronous generator, the rotor of an induction machine does not itself rotate synchronously; it is the "slipping" of the rotor with respect to the synchronous armature

flux that gives rise to the induced rotor currents. Induction generators operate at speeds either higher or lower than the synchronous mechanical speed depending on the slip, which will be given in section 4.2.1.

4.1.3 Linear Generator

A linear electric generator is most commonly used to convert reciprocating (or back-and-forth) motion directly into electrical energy. This shortcut eliminates the need for a crank or linkage that would otherwise be required to convert a reciprocating motion to a rotary motion in order to be compatible with a rotary generator. This is exactly what the oscillating hydrofoil needs. However, the commercial linear generator is very rare and also expensive. At this R&D phase, the ubiquitous commercial rotating generator was employed in the prototype testing. There is an option to customize a linear generator for the oscillating hydrofoil when the oscillating mechanism has been fully verified.

A linear induction generator is basically a rotating electric generator with its stator unrolled and laid out in a line. Instead of driving by rotational motion, it makes use of linear motion along the length of the stator to generate electric current. Figure 4.3 shows a diagram of a linear generator.

There are two design categories of a linear induction generator: low and high acceleration. The low acceleration linear generators are of linear synchronous design. This means the stator has a winding movement on one side of an air gap and a range of alternate pole magnets on the other side. The energy is caused by a moving electromagnetic field applied on conductors. The eddy currents of any conductor appearing on the field will be induced, producing an opposing electromagnetic field. Because the opposing fields distract each other, it forces the conductor to move away, bringing it along the moving magnetic field. This category of linear generator is commonly used in magnetic levitation trains and other ground based transportation such as roller coasters. The stator of this kind of linear generator is quite long and can reach for miles.

The other design category is the high acceleration linear induction generator. The high acceleration linear induction generator is a linear induction design. This means that the stator has an active three phase winding on one side of the air gap and a passive conductor plate on the other side. For our application, the future linear generator should concentrate on a linear induction generator because it allows flexible power control systems to be introduced. For example, the active stator winding current can be precisely controlled by an

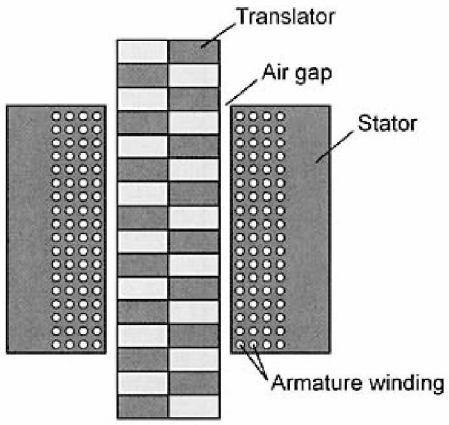

Figure 4.3. Schematic diagram of a linear generator

advanced power control system.

4.2 Micro-Hydro Power Plant Architectures

There are a number of ways to get a constant frequency, constant voltage output from a micro-hydro electric system. Each has its advantages and disadvantages and each should be considered in the design stage of a new power generation system. The fact that one or two methods are most commonly used in hydrokinetic power generation does not mean that the others are impractical in all situations. In oscillating hydrofoil power system design, several of the methods for producing a constant voltage, constant frequency electrical output from a rotating machinery are discussed in this section. They are the Fixed-Speed Induction Generator (FSIG) configuration, Doubly Fed Induction Generator (DFIG) configuration, and Fully Rated Converter based (FRC) configuration. For each configuration, the basic principle is introduced first and the pros and cons when being used by the oscillating hydrofoil system are analyzed. Finally, further recommendations for building the power plant architecture is presented.

4.2.1 Fixed-Speed Induction Generator

Fixed-speed configurations are electrically simple devices consisting of a hydrodynamically driven rotor driving a low-speed shaft, a gearbox, a high-speed shaft and an induction (asynchronous) generator. Refering to the Figure 4.2, it can also represent a schematic diagram of the cross-section of a three-phase induction machine used in FSIG configura-

tion. The stator consists of three-phase windings, *as*, *bs* and *cs*, distributed 120° apart in space. The rotor circuits have three distributed windings *ar*, *br* and *cr*. The angle θ is given as the angle by which the axis of the phase *ar* rotor winding leads the axis of phase *as* stator winding in the direction of rotation and ω_r is the rotor angular velocity in electrical radians per second. The angular velocity of the stator field in electrical radians per second is represented by ω_s. When balanced three-phase currents flow through the stator windings, a field rotating at synchronous speed, ω_s is generated and expressed as

$$\omega_s = \frac{4\pi f_s}{p_f}, \tag{4.1}$$

where f_s (Hz) is the frequency of the stator currents and p_f is the number of poles. If there is relative motion between the stator field and the rotor, voltages of frequency f_r (Hz) are induced in the rotor windings. The frequency f_r is equal to the slip frequency $s \cdot f_s$, where the slip s is given by

$$s = \frac{\omega_s - \omega_r}{\omega_s}. \tag{4.2}$$

The slip is positive if the rotor runs below the synchronous speed and negative if it runs above the synchronous speed [32, 33]. Figure 4.4 [34] shows a simplified equivalent induction machine circuit [35], the simplification is done by moving the magnetizing reactance to the terminals. The power transferred across the air-gap to the rotor (of one phase) is

$$P_{air-gap} = \frac{r_r}{s} I_r^2. \tag{4.3}$$

The torque developed by the machine (one-phase) is given by

$$T_e = \frac{p_f}{2} \frac{r_r}{s\omega_s} I_r^2. \tag{4.4}$$

From the Figure 4.4, the rotor current is

$$\mathbf{I}_r = \frac{\mathbf{V}_s}{(r_s + \frac{r_r}{s}) + j(X_s + X_r)}. \tag{4.5}$$

Then apply Equation 4.4 in three phase, the torque is

$$T_e = 3\frac{p_f}{2}(\frac{r_r}{s\omega_s})\frac{V_s^2}{(r_s + \frac{r_r}{s})^2 + (X_s + X_r)^2}. \tag{4.6}$$

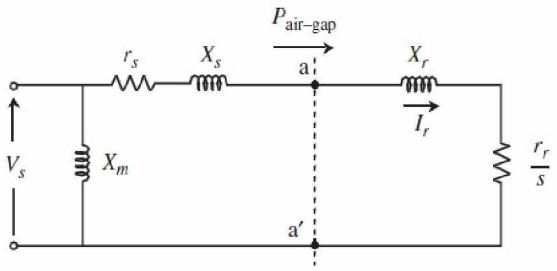

Figure 4.4. Single-phase equivalent circuit of an induction machine for evaluating simple torque - slip relationships

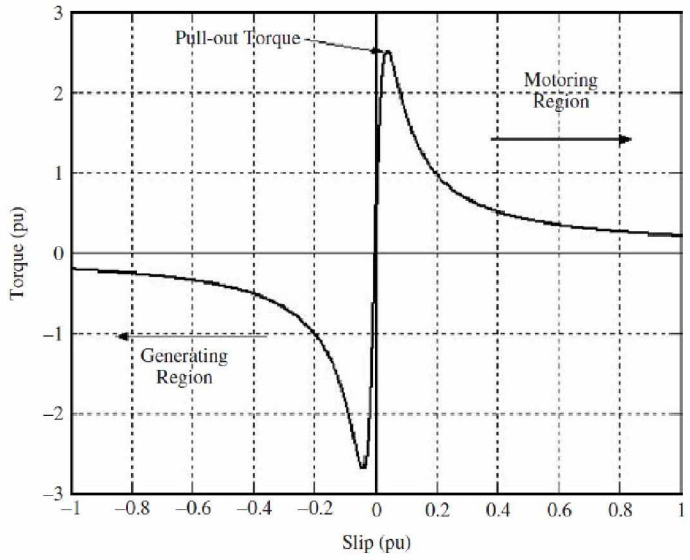

Figure 4.5. Typical torque-slip characteristic of an induction machine

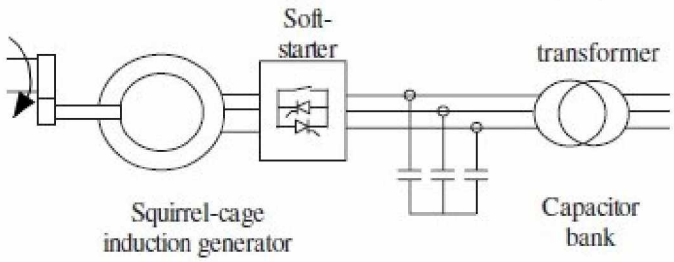

Figure 4.6. Typical configuration of a fixed-speed power system

From Equation 4.6, the relationship between torque and slip is plotted in Figure 4.5 [36]. In a viable speed energy system, this type of operation is normally operated using a squirrel-cage induction generator, wherein the slip varies with the amount of power generated (Figure 4.5). It is not a pure fixed-speed configuration. In most of the wind energy power systems, however, it is normally referred to as a constant speed or fixed-speed power generator configuration because these rotor speed variations are very small $(1-2\%)$ for a wind turbine.

Figure 4.6 illustrates the configuration of a fixed-speed configuration consisting of a squirrel-cage induction generator coupled to the power system through a turbine transformer [34]. The generator operating slip changes slightly as the operating power level changes and the rotational speed is therefore not entirely constant. From the system design point of view, this configuration is the simplest alternative way of implementation used in large turbine or fan systems: drive with torque applied to the low-speed shaft.

Based on the above analysis and the properties of the hydrofoil device, the FSIG configuration is far less dependable in the first place for building a stable and efficient power system for the MHPG system, because the periodic occurrence of the reciprocating motion will cause more speed variations and complicate the power control system in contrast to the wind turbine system. In short, this project turns to another alternative configuration, theDoubly Fed Induction Generator (DFIG), which is more flexible in obtaining a constant output power from a variable speed mechanical power source.

4.2.2 Doubly Fed Induction Generator (DFIG) Configuration

The DFIG configuration is a variable-speed configuration that is widely used in wind turbine systems. In the wind energy industry, as the size of the mechanical motion generation systems becomes larger, the technology has switched from fixed speed to variable speed.

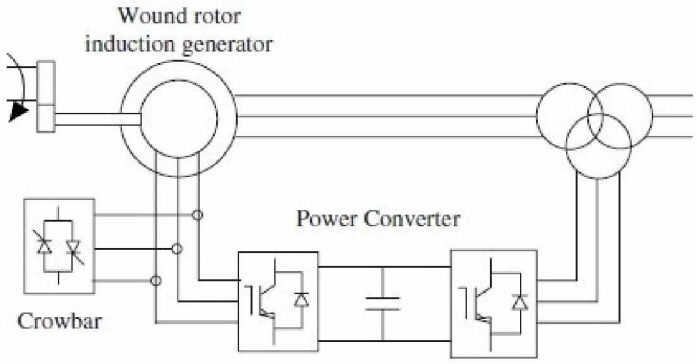

Figure 4.7. Typical configuration of a DFIG power system

The drivers behind these developments are mainly the ability to comply with grid code connection requirements and the reduction in mechanical loads achieved with variable-speed operation. In an oscillating hydrofoil system, it is not a problem to comply with grid codes per se that the system design needs to meet, but with the flexibility that the power systems are capable of in dynamic control and transient fault avoidance.

A typical configuration of a DFIG system is shown schematically in Figure 4.7. It uses a wound-rotor induction generator with slip rings to take current into or out of the rotor winding, and variable-speed operation is obtained by injecting a controllable voltage into the rotor at slip frequency. The rotor winding is fed through a variable-frequency power converter, typically based on two AC/DC IGBT-based voltage source converters (VSCs), and linked by a DC bus. The power converter decouples the network electrical frequency from the rotor mechanical frequency enabling variable-speed operation of the motion generation system. The generator and converters are protected by voltage limits and an over-current "crowbar".

A DFIG wind turbine can transmit power to the network through both the generator stator and the converters. When the generator operates in super-synchronous mode, power will be delivered from the rotor through the converters to the network, and when the generator operates in sub-synchronous mode, the rotor will absorb power from the network through the converters. These two modes of operation are illustrated in Figure 4.8, where ω_s is the synchronous speed of the stator field and ω_r is the rotor speed [35].

The steady state performance can be described using the Steinmetz per phase equiva-

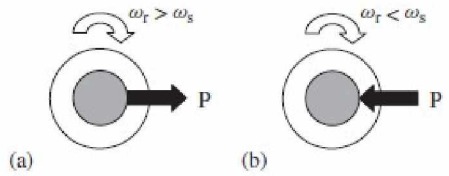

Figure 4.8. (a) Super-synchronous and (b) sub-synchronous operation of the DFIG Generator

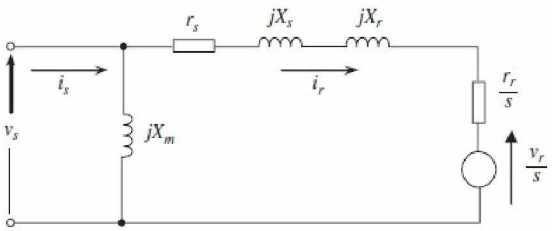

Figure 4.9. Simplified DFIG equivalent circuit with injected rotor voltage

lent circuit model, where motor convention is used [36]. By transferring the magnetising branch to the terminals, the simplified equivalent circuit is shown in Figure 4.9.

The torque - slip curves for the DFIG can be calculated from the approximate equivalent circuit model using the following equations [36]. The rotor current can be calculated from

$$I_r = \frac{V_s - (\frac{V_r}{s})}{(r_s + \frac{r_r}{s}) + j(X_s + X_r)}. \tag{4.7}$$

The electrical torque, T_e, of the machine, which equates to the power balance across the stator to rotor gap, can be calculated from

$$T_e = (I_r^2 \frac{r_r}{s}) + \frac{P_r}{s}, \tag{4.8}$$

where the power supplied or absorbed by the controllable-source injecting voltage into the rotor circuit, that is, the rotor active power, P_r, can be calculated from

$$P_r = \frac{V_r}{s} I_r cos\theta. \tag{4.9}$$

Figure 4.10 shows the power flow in steady-state of a DFIG system. The Table 4.1 presents the parameters used in this figure. The mechanical power and the stator electric power output are computed as follows:

Table 4.1. Representative parameters in Figure 4.10

Parameters	**Meanings**
P_m	Mechanical power captured by the hydrofoil and transmitted to the rotor
P_s	Stator electrical power output
P_r	Rotor electrical power output
P_{gc}	C_{grid} electrical power output
Q_s	Stator reactive power output
Q_r	Rotor reactive power output
Q_{gc}	C_{grid} reactive power output
T_m	Mechanical torque applied to rotor
T_{em}	Electromagnetic torque applied to the rotor by generator
ω_r	Rotational speed of rotor
ω_s	Rotational speed of the magnetic flux in the air-gap of the generator, this speed is named synchronous speed.

$$P_m = T_m \omega_r; \tag{4.10}$$

$$P_s = T_{em} \omega_s. \tag{4.11}$$

For a loss less generator the mechanical equation is:

$$J\frac{d\omega_r}{dt} = T_m - T_{em}. \tag{4.12}$$

In steady state at fixed speed of a loss less generator $T_m = T_{em}$ and $P_m = P_s + P_r$. It follows that:

$$P_r = P_m - P_s = T_m\omega_r - T_{em}\omega_s = T_{em}(\frac{\omega_s - \omega_r}{\omega_s})\omega_s = -sT_m\omega_s = -sP_s, \tag{4.13}$$

where s is defined as the slip of the generator: $S = \frac{\omega_s - \omega_r}{\omega_s}$.

Generally the absolute value of slip is much lower than 1 and consequently the rotor electrical power output P_r is only a fraction of stator real power output P_s. Since the electromagnetic torque T_m is positive for power generation and since ω_s is positive and constant for a constant frequency grid voltage, the sign of P_r is a function of the slip sign. P_r is positive for negative slip (speed greater than synchronous speed) and it is negative

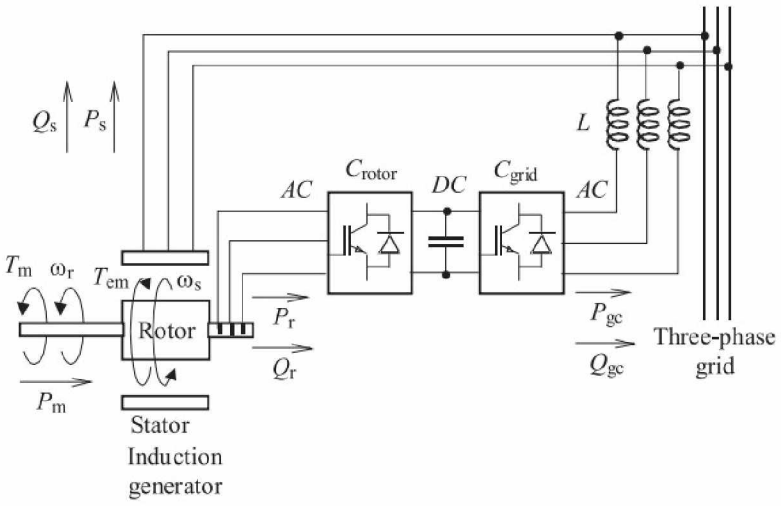

Figure 4.10. Power flow in a DFIG system

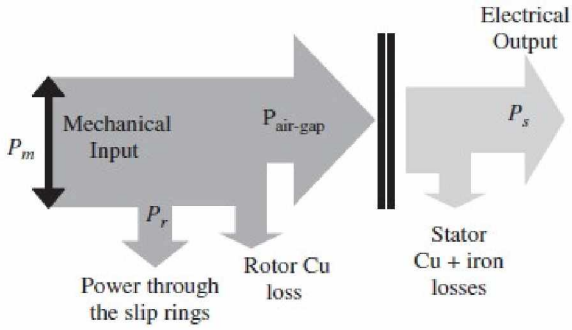

Figure 4.11. Abstract reaction power flow in a DFIG system

for positive slip (speed lower than synchronous speed). For super synchronous speed operation, P_r is transmitted to the DC bus capacitor and tends to raise the DC voltage. For sub synchronous speed operation, P_r is taken out of the DC bus capacitor and tends to decrease the DC bus voltage. The grid side converter is used to generate or absorb the grid electrical power P_{gc} in order to keep the DC voltage constant. In steady state for a lossless AC/DC/AC converter P_{gc} is equal to P_r and the speed of generator rotor is determined by the power P_r absorbed or generated by the rotor side converter. By properly controlling the rotor side converter and the grid side converter using the sensed signal about the dynamics of oscillating hydrofoil, the DC bus voltage of the capacitor can be regulated.

To focus on the active power relationships in the steady state and better understand the efficiency of the DFIG when used in the MHPG system, Figure 4.11 shows the controllable power flow in the MHPG system. In this figure, P_m is the mechanical power delivered by the turbine, P_r is the power delivered by the rotor to the converter, $P_{air-gap}$ is the power at the generator air-gap, P_s is the power delivered by the stator and P_g is the total power generated (by the stator plus the converter) and delivered to the grid.

If the stator losses are neglected, then

$$P_{air\ gap} = P_s, \tag{4.14}$$

and neglecting rotor losses

$$P_{air\ gap} = P_m - P_r. \tag{4.15}$$

So we got the same result of the forgoing analysis that

$$P_s = P_m - P_r. \tag{4.16}$$

It can be expressed in terms of the generator torque, T, as

$$T\omega_s = T\omega_r - P_r, \tag{4.17}$$

where $P_s = T\omega_s$ and $P_m = T\omega_r$. Rearranging terms in Equation 4.17 we get:

$$P_r = -T(\omega_s - \omega_r). \tag{4.18}$$

Then the stator and rotor powers can be related through the slip s as

$$P_r = -sT\omega_s = -sP_s. \tag{4.19}$$

Combining Equation 4.16 and 4.19, the mechanical power, P_m, can be expressed as

$$P_m = (1 - s)P_s, \tag{4.20}$$

and the total power delivered to the grid, P_g, is then given by

$$P_g = P_s + P_r. \tag{4.21}$$

The controllable range of s determines the size of the converters for the DFIG. Mechanical and other restrictions limit the maximum slip and a practical speed range may be between 0.7 and 1.2 pu [35].

4.2.3 Fully Rated Converter (FRC) Configuration

The Fully Rated Converter (FRC) configuration is frequently used in wind turbine constant speed power generation technology. The typical configuration of a fully rated converter system is shown in Figure 4.12. This type of configuration may or may not include a gearbox and a wide range of electrical generator types can be employed, for example, induction, wound-rotor synchronous or permanent magnet synchronous. As all of the power from the mechanical motion goes through the power converters, the dynamic operation of the electrical generator is effectively isolated from the power grid. The electrical frequency of the generator may vary as the motion speed changes, while the grid frequency remains unchanged, thus allowing variable-speed operation of the mechanical motion.

The power converters can be arranged in various ways. Whereas the generator-side converter (GSC) can be a diode rectifier or a PWM voltage source converter (VSC), the network-side converter (NSC) is typically a PWM VSC. The strategy to control the operation of the generator and the power flows to the network depends very much on the type of power converter arrangement employed. The network-side converter can be arranged to maintain the DC bus voltage constant with torque applied to the generator controlled from the generator-side converter. Alternatively, the control philosophy can be reversed. Active power is transmitted through the converters with very little energy stored in the DC link capacitor. Hence the torque applied to the generator can be controlled by the network-side converter. Each converter is able to generate or absorb reactive power independently.

4.3 Summary

In this chapter, an overview of the electric power generator and micro-hydro power plant architectures is presented. Each of the subtopics proposed above deserves to be studied

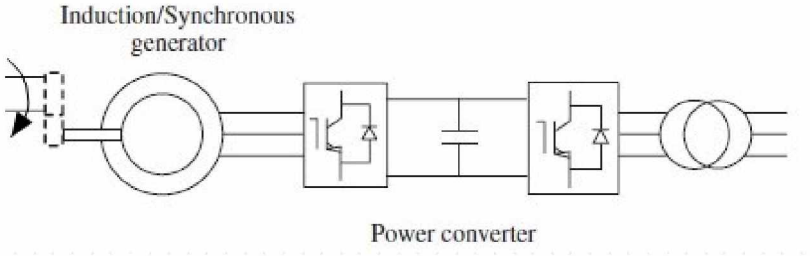

Figure 4.12. Typical configuration of a fully rated converter-connected power system

as a single project in the future in order to enter the commercial phase. Synchronous generators are widely used in fixed speed mechanical power input scenarios, because they offer precise control of voltage and frequency through the use of voltage regulators and governors. Given the fact that the frequency of the voltage developed by synchronous generators depend on the speed of the rotor, it is not appropriate to use synchronous generator in the MHPG system. Asynchronous generators are more appropriate for variable speed power system applications, such as wind turbines. With extra electronic components, asynchronous generators can function as a very flexible power system architecture, which is called the Doubly Fed Induction Generator architecture. By implementing a pair of back to back AC-to-DC and DC-to-AC converters, the rotor output voltage and the grid voltage is decoupled by a DC bus, thus it can work in variable speed operation mode such as the MHPG system. The power control system for MHPG is of paramount importance in producing stable and efficient clean hydro power by an oscillating hydrofoil. The Fixed-Speed Induction Generator architecture and fully rated converter architecture were compared to the DFIG architecture; constant speed operation property of those two power system architectures prevents them from being selected in developing the MHPG system.

The linear generator has also been discussed along with the synchronous and asynchronous generator. It is less popular than the rotating generator and limited in a small amount of applications. The linear generator is the most efficient mechanical-to-electrical power converter for MHPG system, which generates a reciprocal motion from hydrokinetic energy. In the future, the design of linear generator for MHPG system should be delegated to an electronic specialist to directly couple the reciprocating motion of the hydrofoil to the electromagnetic torque of the stator or translator coils.

Chapter 5
Project Device Fabricating and Testing

5.1 Prototype Testing

Aside from the numerical analyses and theoretical designs, a prototype of MHPG system has been built. With an EPSCoR Project Expenses Award sponsored by Alaska EPSCoR program, enough funding was secured to purchase components and fabricate the system. The experiment intended to study an idealized oscillating hydrofoil that is able to generate oscillating motion by flowing water. The system mainly consists of three links: a long rigid rod, which is able to rotate around a fixed point at one end; a large wing-like hydrofoil with cord length of 50 cm and vertical width about 60 cm, which is connected with a hinge to the other end of the rod; and a deflected flap, or trim tab, the orientation of which can be controlled by a linear actuator. The three rigid links are connected by rotational joints (Figure 5.1). The hydrofoil was fabricated according to the standard NACA0009 foil, so that the experimental data collected from the prototype test can be compared to the numerical results from simulation of a standard NACA0009 foil. The difference will be used to improve our modeling process and optimize the prototype.

Figures 5.2 is the 3D design of the linear-to-rotational motion conversion subsystem, which is mainly a modified Scotch Yoke mechanism. The rotational part in the Scotch Yoke mechanism is the spur gear, which will be driven by the rod from the oscillating motion generation system. The output of this gear will be coupled with a smaller gear which will directly connect to the electric power generator (Figure 5.3).

The first field experiment was conducted in October 2010. The goal during the iinitial primary test was to verify the original ideas by showing that the foil can move back and forth under the fluid force. The static force acting on the hydrofoil system was also studied. From this test we gained confidence about the concepts of the oscillating hydrofoil power generating system. By manually controlling the trim tab, an oscillating motion was observed. What was also observed is that the motion of the hydrofoil under fluid force is very sensitive to the deflected angle of the trim tab. It required some time before a manual operator could control the trim tab in order to generate a stable oscillating motion by the hydrofoil in the flowing water. In the future, the trim tab control will be handled by a well designed digital control system. The first test configuration is show in the Figure 5.4.

With the Alaska EPSCoR Travel Award and the Project Expenses Award, a scientific collaborative travel to California became possible. The project collaborator, Mr. Robert

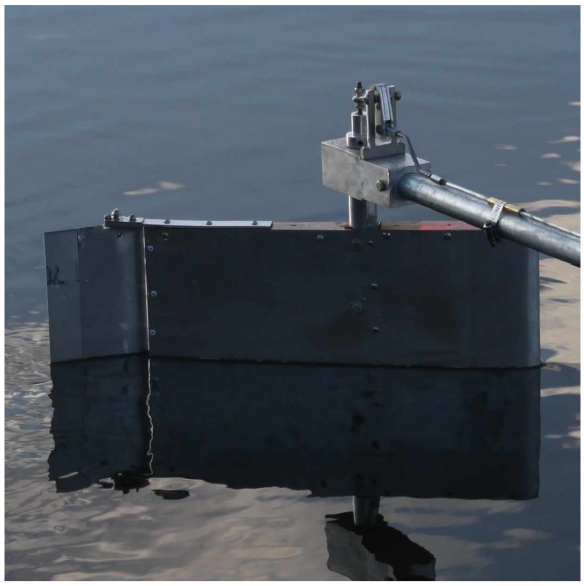

Figure 5.1. Prototype of the hydrofoil in a field test

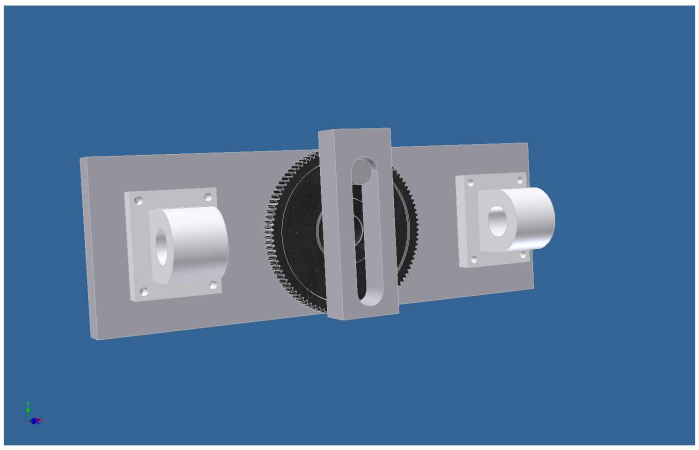

Figure 5.2. 3D design of the Scotch Yoke in Autodesk® Inventor

Figure 5.3. Hurricane Water Works micro-hydro generator from Hurricane Windpower

Figure 5.4. Configuration of the first river test of the prototype hydrofoil

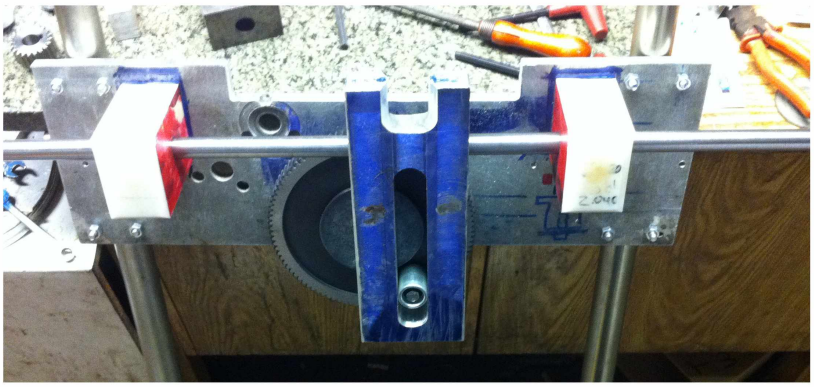

Figure 5.5. Fabricated linear-to-rotational motion translation system

Palmer, is a mechanist and the owner of the "prototype factory". With the help from Mr. Palmer, the linear-to-rotational motion conversion system was fabricated and coupled with the oscillating generating subsystem at the "prototype factory".

Figure 5.5 shows the prototype of the linear-to-rotational motion conversion system. All the bearings of the system were natural bearing because they were easy to make, and we were looking for the simplest solution at this stage of development. We tested the mechanism of the prototype and observed a potential problem when the Scotch Yoke was used as part of our oscillating hydrofoil system. The problem is that when the oscillating motion comes down to very slow speeds, the linear motion part of the "Scotch Yoke" will stall at the left most or right most point. Further improvement to the Scotch Yoke will be made in the future, such as modifying the shape of the slot and embedded springs in the slot, to reduce the chance of stall.

In the California River test, a commercial linear actuator was employed to control the orientation of the trim tab (See Figure 5.6). With the precise design of the commercial control box and the actuator, much smooth and stable oscillating motions were observed. The river flow's velocity was measured, and it was equal to 0.75 m/s. In addition, the pull of the hydrofoil was also measured using a 50-pound scale. The maximum pull of 147 Newton measurement result was read when the Angle of Attack was equal to approximately 10°. This result is similar to the numerical results we get in Figure 3.8.

The final prototype of the MHPG system is shown in the Figure 5.7, and Figure 5.8 shows the details of how the electric power generation system has been coupled. There are several problems with this prototype when it was tested in a river. First, the mechanical transmission system is overloaded for the natural bearing we used; it is very hard to

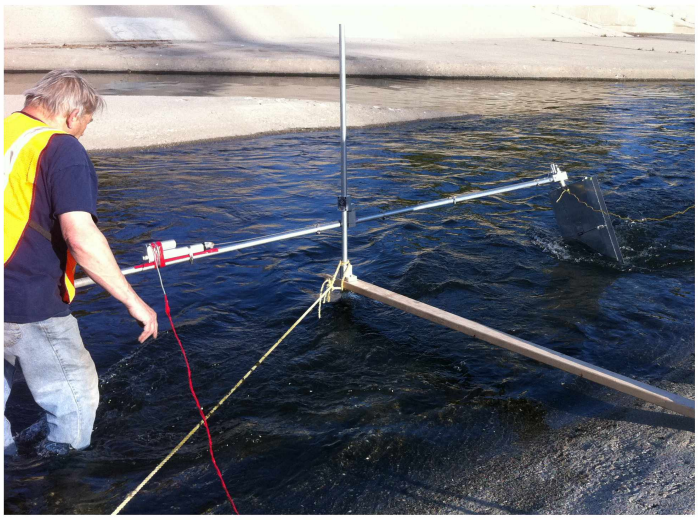

Figure 5.6. Configuration of the second river test of the prototype hydrofoil

complete the transient motion at the right most position or left most position. Secondly, the Scotch Yoke system needs to be further modified to conquer the lock-in point when the oscillation motion is very slow. The next phase of prototype development will focus on improving the bearing system and will try to deploy a larger foil system as the driver.

In the future, the theoretical and experimental study of the oscillating hydrofoil system should go hand in hand with one another. Because concrete performance data of the MHPG system should be obtained under several different flow velocities, a laboratory water duct with controllable flowing velocity may need to be constructed. The hydrofoil may also need to be modified or even reconfigured with multiple sensors. Such sensors can measure the dynamic displacement or acceleration of the oscillating foil when the system is configured to alternate the orientation of the trim tab. The dynamic displacement and the dynamic acceleration of the hydrofoil are very important experimental data that can be used to estimate the capacity of MHPG system.

Figure 5.7. Final prototype of the oscillating hydrofoil power generation system

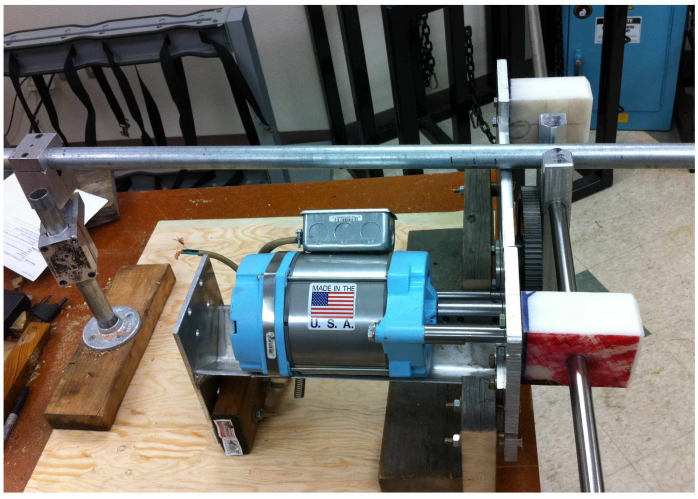

Figure 5.8. Electric power generator coupling in the final prototype of MHPG system

Chapter 6
Conclusion and Future Work

At the beginning chapter of this thesis, a literature review about sustainable energy development and overviews of how government policies and regulation will benefit research and development of clean energy technologies were presented. In chapter two, eleven hydrokinetic power generation projects and the technologies these projects used have been reviewed and evaluated on a case by case discussion. The advantages and disadvantages of those technologies have also been investigated. Chapter three introduces the oscillating hydrofoil power generation system, which was first invented and patented by one of our group members Robert C. Kallenberg. The mathematical description of the oscillating hydrofoil model is derived, and further discussion about how those mathematics problems can be solved by COMSOL Multiphysics software is also provided. Before solving the models, the Computational Fluid Dynamics CFD module in COMSOL is introduced. Because simulating a hinge in a fluid using the method of finite element analysis is complex, an analytical method is used first to study how the foil will move under fluid force. Secondly, COMSOL is used to solve the quantitative results in the discrete scenarios. In a river with an average speed of 1 m/s, our measurements show that the maximum pull of 500 Newton can be generated to drive the mechanical-to-electrical power converter, such as a permanent magnetic generator. Based on the analysis of the obtained results, the idea of studying the hydrofoil system as a trajectory planning robot is proposed. Because COMSOL is only capable of solving problems that involve only the fluid structure interaction, the dynamics of the oscillating system should be studied separately. This idea points out a potential working direction for the future development of the oscillating hydrofoil system.

A mechanism called Scotch Yoke has been proposed to undertake the linear to rotational motion conversion in the MHPG system. A Scotch Yoke was machined to the requirement of the prototype. This mechanism works well most of the time, except when the motion of the foil is extremely slow due to the low flow speed.

Chapter 4 initiated the design of the electrical power system for the MHPG system. The theory of the synchronous power generator, the asynchronous power generator, and the linear power generator are introduced and analyzed with respect to the operation of the oscillating hydrofoil. Following that, three different hydrokinetic power system configurations are analyzed in detail. The first configuration is the FSIG configuration, in which the deployment of the oscillating hydrofoil system is assumed not to be connected to any local

grid or regional power networks. The second type configuration is Double Fed Induction Generator (DFIG) configuration. The DFIG is widely used in wind turbine systems, its transient property can be designed according to the motion generating system properties. That means the dynamics of the motion generation system should be explicitly studied, and the data obtained can be fed into a feed back control loop in the operating process. Even though the input torque is variable, the DFIG can produce constant output electricity with proper power converter control techniques. Future work should be dedicated to studying the transient properties of the DFIG and its performance under network fault or hydrofoil fault.

There are still many directions in which this work should proceed. First of all, the transient analysis of the hydrofoil in the left most position or right most position should be further studied. Research on how the motion of the controllable trim tab will effect the fluid torque on the hydrofoil, and how the oscillating motion generation system will be changed under such effect, should be further addressed. Secondly, when the hydrodynamics of the "in-stream" hydrofoil has been fully studied, the time dependent data obtained from hydrodynamic modeling can be imported as the necessary data to initiate the iterative Newton - Euler dynamics algorithm, which was discussed in chapter three. The closed form of Newton - Euler dynamics algorithm can be used to solve the displacement, velocity, and acceleration of both the hydrofoil and the support rod. For the Scotch Yoke, the "dead point" problem in mechanical design of our linear-rotational motion conversion system should be alleviated. While this "dead point" issue is tolerable in the test phase, it should be eliminated when the design becomes mature and goes into the pre-commercial phase. Moreover, the power electronic system's performance is greatly determined by the motion of the hydrofoil. The system integration study about the relationships between the parameters of the hydrofoil and the performance of the power system should be studied in depth. This requires investigations in fluid dynamics, finite element analysis modeling, power electronics, and system engineering. To that end, the project should be pursued by a diverse team of experts in each of these fields in the future.

Bibliography

[1] J. J. Conti, P. D. Holtberg, J. A. Beamon, A. M. Schaal, G. E. Sweetnam, A. S. Kydes, et al. Annual Energy Outlook 2010. Technical report, Energy Information Administration, April 2010.

[2] JREN21. Renewables 2007 Global Status Report. Technical report, REN21 Secretariat and Washington,DC: Worldwatch Institute, 2008.

[3] JREN21. Renewables 2010 Global Status Report. Technical report, Paris: REN21 Secretariat, 2010.

[4] R. Bedard, M. Previsic, G. Hagerman, B. Polagye, W. Musial, B. Roger, et al. In *Proceedings of the 7th European Wave and Tidal Energy Conference*, Porto, Portugal, September 2007.

[5] D. Dixon. The Future of Waterpower: 23,000 MW+ by 2025. Technical report, EPRI, Environment and Energy Study Institute briefing. Washington, DC, April 2008.

[6] U. of Concerned Scientists. How Hydrokinetic Wroks, April 2008.

[7] D. of Energy. Hydrokinetic Projects, http://www.ferc.gov/industries/hydropower/indus-act/hydrokinetics/issued-hydrokinetic-permits-map.pdf.

[8] DIT. The Engineering Business: Research and Development of a 150 kW Tidal Stream Generator Phase 1. Technical report, The Engineering Business Limited, 2002.

[9] DIT. The Engineering Business: Research and Development of a 150 kW Tidal Stream Generator Phase 2. Technical report, The Engineering Business Limited, 2003.

[10] DIT. The Engineering Business: Stingray Tidal Stream Energy Device Phase 3. Technical report, The Engineering Business Limited, 2005.

[11] A. H. E. R. C. (AHERC). Alaska Hydrokinetic Research Center (AHERC) DRAFT STRATEGIC PLAN 2010 - 2013, 2010.

[12] P. Crimp, M. Devine, D. Lockard, R. Loewen, J. Jensen, D. Ott, et al. Renewable Energy Altas of Alasak. Technical report, Alaska Energy Authority and Renewable Energy Alaska Project (REAP), May 2009.

[13] G. Holdmann, S. Haagenson, A. Byrd, G. Fay, N. Symoniak, S. Colt, et al. Alaska Energy - A first step toward energy independence. Technical report, Alaska Energy Authority and Alaska Center for Energy and Power, January 2009.

[14] R. C. K. Jr. Hydrodynamic Power-Generating System. US6323563, November 2001.

[15] M. Platzer and J. Ekaterinaris. ASME FEDSM99-7050, San Francisco, July 1999. 3rd ASME/JSME Joint Fluids Engineering Conference.

[16] M. Platzer and J. Ekaterinaris. *An Investigation of the Fluid-Structure Interaction in an Oscillating-Wing Micro-Hydropower Generator*, volume Fluid Structure Interaction II, pages 73–84. WIT Press, 2003.

[17] M. M. Bernitsas, K. Raghavan, Y. Ben-Simon, and E. M. H. Garcia. *Journal of Offshore Mechanics and Arctic Engineering*, 130(4):041101, 2008.

[18] B. Hirsch and M. Worthington. In-Stream Hydrokinetic Turbine in Ruby, Alaska. Technical report, YRITWC Energy Department, 2008.

[19] B. Grimm. The Yukon River hydrokinetic turbine project Eagle, Alaska. Technical report, Alaska Power & Telephone Company, 2008.

[20] Igiugig Electric Hydropower Scoping Brief. Technical report, Igiugig Village Council, 2007.

[21] H. W. Group, Online: http://www.akenergynetwork.com/.

[22] O. C. P. System, Online: http://www.arnoldenergysystems.com/index.html.

[23] C. E. Commission, Online: http://www.energy.ca.gov/.

[24] D. of Energy, Online: http://www.energy.gov/.

[25] M. T. Pontes and A. Falcao. In *Proceedings of 18th WEC Congress*, Buenos Aires, Oct. 2001.

[26] European Wave Energy Thematic Network. Technical report, WaveNet, 2003.

[27] An Overview of Wave Energy Technologies. Technical report, Future Energy Solutions, 1998.

[28] Wave Energy Project Results: The Exploitation of Tidal Marine Currents. Technical report, Commission of the European Com, 1996.

[29] Status and Research and Development Priorities 2003: Wave and Marine Current Energy. Technical report, International Energy Agency - Ocean Energy Systems.

[30] C. AB. COMSOL CFD Module Users Guide, October 2010 COMSOL 4.1.

[31] J. J. Craig. *Introduction to Robotics Mechanics and control*. Prentice Hall, 3rd edition, 2005.

[32] P. Kundur. *Power System stability and control*. McGraw-Hill, New York, 1994.

[33] P. Krause, O. Wasynczuk, and S. D. Shudhoff. *Analysis of Electric Machinery and Drive System*. Wiley-IEEE Press, New York, 2002.

[34] N. D. Caliao. *Renewable Energy*, 36(8):2287 – 2297, 2011.

[35] B. Fox, D. Flynn, L. Bryans, N. Jenkins, M. Milborrow, D.and OMalley, R. Watson, and O. Anaya-Lara. *IET Power and Energy Series*, Vol. 50, 2007.

[36] J. Hindmarsh. *Electrical Machines and Their Applications*. Butterworth-Heinemann, Oxford, 1995.